# Spin-lattice interaction parameters from first principles: Theory and implementation

Sergiy Mankovsky⬤, Hannah Lange⬤, Svitlana Polesya⬤, and Hubert Ebert⬤

*Department of Chemistry/Phys. Chemistry, LMU Munich, Butenandtstrasse 11, D-81377 Munich, Germany*

A scheme is presented to calculate on a first-principles level the spin-lattice coupling (SLC) parameters needed to perform combined molecular-spin dynamics (MSD) simulations. By treating changes to the spin configuration and atomic positions on the same level, closed expressions for the atomic SLC parameters could be derived in a coherent way up to any order. The properties of the SLC parameters are discussed considering separately the symmetric and antisymmetric parts of the SLC tensor. The changes due to atomic displacements of the spin-spin exchange coupling (SSC) parameters estimated using the SLC parameters are compared with the SSC parameters calculated for an embedded cluster with the central atom displaced, demonstrating good agreement of these results. Moreover, this allows to study the impact of different SLC contributions, linear and quadratic with respect to displacements, on the properties of the modified SSC parameters. In addition, we represent an approach to calculate the site-diagonal SLC parameters characterizing local magnetic anisotropy induced by a lattice distortion, which is a counterpart of the approach based on magnetic torque used for the investigations of magneto-crystalline anisotropy (MCA) as well as for calculations of the MCA constants. In particular, the dependence of the induced magnetic torque on different types of atomic displacements is analyzed.

## I. INTRODUCTION

While the ground state of magnetic materials is reasonably well described within the spin density functional theory (SDFT) based first-principles approach, the Heisenberg model is a tool giving access to the finite temperature and nonequilibrium magnetic properties, making use of Monte Carlo [1] or spin-dynamics simulations [2], which are successfully applied both to materials with robust local magnetic moment as well as to metallic systems often treated as non-Heisenberg. In this context it is important to note that it was a challenge for many years to describe the thermodynamics of metallic magnetic materials on the basis of the Heisenberg model [3,4] with the corresponding coupling parameters derived using model electron Hamiltonians. Later on first-principles calculations of the exchange coupling parameters $J_{ij}$ done within the framework of SDFT have been reported by various groups [5–12]. This way a variety of systems including nonmetallic ones [6] could be studied although the leading mechanisms of the exchange interaction in these materials may be different, depending on their structure and composition (more details can be found in recent review articles [13,14]). A very efficient nonrelativistic approach for calculations of the exchange coupling parameters, based on the magnetic force theorem (MFT), was suggested by Lichtenstein *et al.* [7], giving an explicit expression on the basis of the multiple scattering formalism. Corresponding extensions of this computational scheme are now available to account for the full tensorial form of the interaction parameters [15,16] as well as their extension to a multisite formulation [17,18].

However, a description of magnetic properties based on a spin Hamiltonian, in general, is incomplete, as it does not take into account spin-lattice or magnetoelastic interactions. For some materials, a corresponding contribution to the Hamiltonian may be neglected because of a negligible spin-lattice coupling (SLC) while this is not the case for systems with strong spin-lattice interactions, which may be responsible for various interconnected magnetic and structural properties. This concerns, for instance, a structural transformation accompanying the magnetic ordering transition observed in noncollinear antiferromagnets $R$MnO$_3$ [19] (where $R$ is a rare-earth element), CuCrO$_2$ [20], CuCrS$_2$ [21], and AgCrS$_2$ [22], as well as a formation of collinear order with complex structure in triangular lattice antiferromagnets exhibiting strong geometrical frustration because of antiferromagnetic nearest-neighbor exchange interactions [23,24]. A sufficiently strong spin-lattice coupling may be responsible for the magnon-phonon hybridization leading to mutual modifications of both the magnon and phonon spectra that have been found in experiments on the noncollinear antiferromagnets CuCrO$_2$ [25] and (Y,Lu)MnO$_3$ [26,27]. Recent investigations on ultrafast demagnetization [28–30] demonstrate the importance of SLC for angular momentum transfer between the spin and lattice subsystems, which may play a crucial role for the ultrafast demagnetization [31–34]. Some phenomena determined by magnon-phonon coupling are expected to be useful for various applications, e.g., in spintronics. This for example holds for the inverse Edelstein effect, which implies spin to charge current conversion with a spin current generated by a surface acoustic wave in a ferromagnetic layer via magnon-phonon coupling [35]. Here one can also mention the possibility to drive efficiently magnetic bubble domain walls, skyrmions, and magnetic vortices by magnetoelastic waves [36], which is of great practical importance for insulating materials when compared to metallic systems where domain walls can be moved by spin currents. A rapidly growing interest is also

in the optical switching of the magnetization driven by spin-lattice coupling [37,38].

Obviously, the growing interest in SLC driven magnetic properties and phenomena already motivated many investigations on the mutual influence of the spin and lattice degrees of freedom. Most of the investigations on magneto-elastic properties have been performed so far on the basis of the phenomenological continuous-field theory [39–41] using parameters derived from experiment. More recent work is based on results from first-principles electronic structure calculations, as for instance the magnetism-driven structure transformations (see e.g., [42,43] and references therein), spin-dynamic simulations using temperature dependent exchange coupling parameters modified due to thermal lattice vibrations [18,44,45], or mutual spin and lattice thermodynamic properties combining quantum Monte Carlo simulations for the spin degree of freedom combined with DFT-based force constant calculations [46]. Obviously, combined molecular-spin dynamics (MSD) simulations [34,47–50] give access to the central aspects of the above mentioned interesting and challenging experiments and phenomena. A corresponding scheme required to calculate the necessary SLC parameters on the basis of electronic structure calculations has been suggested by Hellsvik *et al.* [51] and Sadhukhan *et al.* [52]. Within this approach the standard Lichtenstein formula for the exchange coupling constant is applied to a system with an atom displaced from its equilibrium position and represented by a super cell. In the following we present an alternative scheme that treats changes to the spin configuration and atomic positions on the same level by applying a corresponding extension to the Lichtenstein formula [53]. This allows to derive closed expressions for the atomic SLC parameters in a coherent way up to any order, followed by MSD simulation [54] making use of these parameters.

Furthermore, we present a scheme to calculate the site-diagonal SLC parameters characterizing local magnetic anisotropy induced by a lattice distortion. It follows the approach suggested by Wang *et al.* [55], giving access to the magnetic anisotropy via the calculation of the magnetic torque, which accounts for all contributions to the magnetocrystalline anisotropy (MCA). Moreover, it allows to calculate in an efficient way all MCA constants entering the spin Hamiltonian. A more general expression was worked out by Staunton *et al.* on the basis of multiple scattering theory [56]. Below we use a similar idea to calculate the MCA-like contributions in the spin-lattice Hamiltonian. It should be mentioned that in a complementary paper [57] we consider in addition the role of the classical dipole-dipole interaction for the SLC. Furthermore, this paper presents and discusses further numerical results for various 2D and 3D materials, in particular the magnetic films and compounds which magnetic properties are strongly determined by prominent magnetic frustrations and spin-lattice interactions.

## II. INTERSITE SPIN-LATTICE INTERACTIONS

### A. Spin-lattice Hamiltonian

To describe the coupling of the spin and spatial degrees of freedom, i.e., between the spin and lattice subsystems we adopt an atomistic approach and start with the phenomenological spin-lattice Hamiltonian

$$
\begin{aligned}
\mathcal{H}_{SLC} = & -\sum_{\substack{i,j,\alpha,\beta \\ k,\mu}} \mathcal{J}_{ij,k}^{\alpha\beta,\mu} e_i^\alpha e_j^\beta u_k^\mu - \sum_{\substack{i,j,\alpha,\beta \\ k,l,\mu,\nu}} \mathcal{J}_{ij,kl}^{\alpha\beta,\mu\nu} e_i^\alpha e_j^\beta u_k^\mu u_l^\nu \\
& + \sum_{\substack{i,\alpha,\beta \\ k,\mu}} \mathcal{K}_{i,k}^{\alpha\beta,\mu} e_i^\alpha e_i^\beta u_k^\mu + \sum_{\substack{i,\alpha,\beta \\ l,k,\mu\nu}} \mathcal{K}_{i,kl}^{\alpha\beta,\mu,\nu} e_i^\alpha e_i^\beta u_k^\mu u_l^\nu ,
\end{aligned}
$$
(1)

that can be seen as an extension of the standard Heisenberg spin Hamiltonian. Accordingly, the spin and lattice degrees of freedom are represented by the orientation vectors $\vec{e}_{i(j)}$ of the magnetic moments $\vec{M}_{i(j)}$ on the site $i(j)$, and atomic displacement vectors $\vec{u}_{k(l)}$ for the atomic site $k(l)$. In Eq. (1) we omitted the spin-spin coupling (SSC) terms as well as the elastic interaction term represented by the interatomic force constants [51], as we focus here on the SLC parameters and their properties. Moreover, the spin-lattice coupling has been restricted to three and four-site terms in Eq. (1) (terms 1 and 2) $\mathcal{J}_{ij,k}^{\alpha\beta,\mu}$ and $\mathcal{J}_{ij,kl}^{\alpha\beta,\mu\nu}$, described in tensorial form as relativistic effects are taken into account. The parameters $\mathcal{K}_{i,k}^{\alpha\beta,\mu}$ and $\mathcal{K}_{i,kl}^{\alpha\beta,\mu\nu}$ characterize the local magnetic anisotropy arising on site $i$ due to displacements of surrounding atoms $k$ and $l$. The Hamiltonian in Eq. (1) that is similar in form to that suggested by Hellsvik *et al.* [51] obviously provides a suitable basis for advanced MSD simulations.

### B. Calculation of the $J_{ij,k}^{\alpha\beta,\mu}$ parameters

In previous works expressions for the nonrelativistic and relativistic exchange coupling parameters $J_{ij}$ [7] or $J_{ij}^{\alpha\beta}$ [15,16], respectively, have been derived by mapping the free energy landscape $F(\{\vec{e}_i\})$ obtained from first-principles electronic structure calculations on the Heisenberg spin Hamiltonian. Here we follow the same strategy by mapping the free energy landscape $F(\{\vec{e}_i\}, \{\vec{u}_i\})$ by accounting for its dependency on the spin configuration $\{\vec{e}_i\}$ as well as atomic displacements $\{\vec{u}_i\}$ on the same footing. Making use of the magnetic force theorem the change in free energy $\Delta F$ induced by changes of the spin configuration $\{\vec{e}_i\}$ with respect to a suitable reference system and simultaneous finite atomic displacements $\{\vec{u}_i\}$ may be written in terms of corresponding changes to the single-particle energies [7],

$$
\Delta F = - \int^{E_F} dE \, \Delta N(E) ,
$$
(2)

where $E_F$ is the Fermi energy and $\Delta N(E)$ is the change to the integrated density of states (NOS); see e.g., Eq. (6) in Ref. [7].

The use of the magnetic force theorem when calculating the conventional exchange coupling parameters $J_{ij}$ via the LKGA scheme turned out to be rather successful for a wide spectrum of materials, as can be seen from numerous reports in the literature (see for instance the recent review articles [13,14]). At the same time, one has to keep in mind also its restrictions and their possible impact on the results based on it; an issue also widely discussed and documented in the literature [7,14,58–61]. When dealing with the SLC param-

eters one has obviously a similar situation that gets more complex as it involves not only the spin but also the lattice degree of freedom. To justify the use of the magnetic force theorem or more general of Andersen's force theorem also here we point out that spin tilting and atomic displacements can be seen as independent perturbations allowing to consider their impact in two steps one after the other (see, e.g., Ref. [62]). A further justification can obviously be achieved by comparing numerical results for the SLC parameters obtained when using the scheme sketched here and those obtained by more accurate but more time consuming methods [51,53]. A corresponding comparison will be presented below (see also Refs. [53,57]).

As exploited before [7,15,16], $\Delta N(E)$ can be evaluated in a very efficient way via the so-called Lloyd formula when the underlying electronic structure is described by means of the multiple scattering or KKR (Korringa-Kohn-Rostoker) formalism (see Appendix B) [63]. Adopting this approach one has

$$\Delta F = -\frac{1}{\pi} \text{Im Tr} \int^{E_F} dE \left( \ln \underline{\underline{\tau}}(E) - \ln \underline{\underline{\tau}}^0(E) \right), \quad (3)$$

with $\underline{\underline{\tau}}^{(0)}(E)$ the so-called scattering path operator, where the double underline indicates matrices with respect to site and spin-angular momentum indices [63]. Within the KKR formalism these super matrices characterizing the reference $(\underline{\underline{\tau}}^{(0)}(E))$ and perturbed $(\underline{\underline{\tau}}(E))$ systems, respectively, are given by

$$\underline{\underline{\tau}}^{(0)}(E) = [\underline{\underline{m}}^{(0)}(E) - \underline{\underline{G}}(E)]^{-1}, \quad (4)$$

with $\underline{\underline{G}}(E)$ the structure Green's function and $\underline{\underline{m}}^{(0)}(E) = [\underline{\underline{t}}^{(0)}(E)]^{-1}$ the inverse of the corresponding site-diagonal scattering matrix that carries all site-specific information depending on $\{\vec{e}_i\}$ and $\{\vec{u}_i\}$ [63].

Considering a ferromagnetic reference state ($\hat{e}_i = \hat{e}_z$) with all atoms in their equilibrium positions ($\vec{u}_i = 0$) the perturbed state is characterized by finite spin tiltings $\delta\hat{e}_i$ and finite atomic displacements of the atoms $\vec{u}_i$ for the sites $i$. Writing for site $i$ the resulting changes in the inverse t-matrix as $\Delta^s_\alpha \underline{m}_i = \underline{m}_i(\delta\hat{e}^\alpha_i) - \underline{m}^0_i$ and $\Delta^u_\nu \underline{m}_i = \underline{m}_i(u^\nu_i) - \underline{m}^0_i$ allows to replace the integrand in Eq. (3) by

$$\ln \underline{\underline{\tau}} - \ln \underline{\underline{\tau}}^0 = -\ln\left(1 + \underline{\underline{\tau}} \left[ \Delta^s_\alpha \underline{m}_i + \Delta^u_\nu \underline{m}_j + ... \right]\right), \quad (5)$$

where all site-dependent changes in the spin configuration $\{\vec{e}_i\}$ and atomic positions $\{\vec{u}_i\}$ are accounted for in a one-to-one manner by the various terms on the right-hand side. This implies in particular that the matrices $\Delta^s_\alpha \underline{m}_i$ and $\Delta^u_\nu \underline{m}_i$ in Eq. (5) are site-diagonal and have nonzero blocks only for site $i$. Assuming small tilting and displacement amplitudes leading in turn to small changes of inversed scattering matrix $\Delta^s_\alpha \underline{m}_i$ and $\Delta^u_\nu \underline{m}_i$, a Taylor series expansion for the logarithm function in Eq. (5) gives access to the terms having different order with respect to the spin tilting and atomic displacement. Making use of the magnetic force theorem, these blocks may be written in terms of the spin tilting $\delta\hat{e}^\alpha_i$ and atomic displacements of the atoms $u^\mu_i$ together with the corresponding auxiliary matrices $\underline{T}^\alpha_i$ and $\mathcal{U}^\mu_i$,

respectively, as

$$\Delta^s_\alpha \underline{m}_i = \delta\hat{e}^\alpha_i \, \underline{T}^\alpha_i, \quad (6)$$

$$\Delta^u_\mu \underline{m}_i = u^\mu_i \, \underline{\mathcal{U}}^\mu_i, \quad (7)$$

which represent the terms linear with respect to perturbations $\delta\hat{e}^\alpha_i$ and $u^\mu_i$ (for more details see Appendix C). Inserting these expressions into Eq. (5) and the result in turn into Eq. (3) allows in a straight forward way to calculate the parameters of the spin-lattice Hamiltonian as the derivatives of the free energy with respect to tilting angles and displacements. This way, accounting for the "minus" sign in the Hamiltonian in Eq. (1), and using the third- and fourth-order terms of the Taylor series in Eq. (5), one obtains for the SLC parameters up to fourth order the general expressions

$$\mathcal{J}^{\alpha\beta,\mu}_{ij,k} = -\frac{\partial^3 \mathcal{F}}{\partial e^\alpha_i \, \partial e^\beta_j \, \partial u^\mu_k} = -\frac{1}{2\pi} \text{Im Tr} \int^{E_F} dE$$
$$\times \left[ \underline{T}^\alpha_i \, \underline{\tau}_{ij} \underline{T}^\beta_j \, \underline{\tau}_{jk} \underline{\mathcal{U}}^\mu_k \, \underline{\tau}_{ki} + \underline{T}^\alpha_i \, \underline{\tau}_{ik} \underline{\mathcal{U}}^\mu_k \, \underline{\tau}_{kj} \underline{T}^\beta_j \, \underline{\tau}_{ji} \right] \quad (8)$$

and

$$\mathcal{J}^{\alpha\beta,\mu\nu}_{ij,kl} = -\frac{\partial^4 \mathcal{F}}{\partial e^\alpha_i \, \partial e^\beta_j \, \partial u^\mu_k \partial u^\nu_l} = \frac{1}{2\pi} \text{Im Tr} \int^{E_F} dE$$
$$\times \left[ \underline{T}^\alpha_i \, \underline{\tau}_{ij} \underline{T}^\beta_j \, \underline{\tau}_{jk} \underline{\mathcal{U}}^\mu_k \, \underline{\tau}_{kl} \underline{\mathcal{U}}^\nu_l \, \underline{\tau}_{li} \right.$$
$$+ \underline{T}^\alpha_i \, \underline{\tau}_{ij} \underline{T}^\beta_j \, \underline{\tau}_{jl} \underline{\mathcal{U}}^\mu_l \, \underline{\tau}_{lk} \underline{\mathcal{U}}^\nu_k \, \underline{\tau}_{ki}$$
$$+ \underline{T}^\alpha_i \, \underline{\tau}_{il} \underline{\mathcal{U}}^\nu_l \, \underline{\tau}_{lj} \underline{T}^\beta_j \, \underline{\tau}_{jk} \underline{\mathcal{U}}^\mu_k \, \underline{\tau}_{ki}$$
$$+ \underline{T}^\alpha_i \, \underline{\tau}_{ik} \underline{\mathcal{U}}^\mu_k \, \underline{\tau}_{kj} \underline{T}^\beta_j \, \underline{\tau}_{jl} \underline{\mathcal{U}}^\nu_l \, \underline{\tau}_{li}$$
$$+ \underline{T}^\alpha_i \, \underline{\tau}_{ik} \underline{\mathcal{U}}^\mu_k \, \underline{\tau}_{kl} \underline{\mathcal{U}}^\nu_l \, \underline{\tau}_{lj} \underline{T}^\beta_j \, \underline{\tau}_{ji}$$
$$\left. + \underline{T}^\alpha_i \, \underline{\tau}_{il} \underline{\mathcal{U}}^\nu_l \, \underline{\tau}_{lk} \underline{\mathcal{U}}^\mu_k \, \underline{\tau}_{kj} \underline{T}^\beta_j \, \underline{\tau}_{ji} \right], \quad (9)$$

that supply the basis for corresponding calculations of the SLC parameters [53]. In the following these terms will be called three- and four-site SLC terms, respectively, even if the site indices are identical. Note that the site-diagonal parameters, e.g., $\mathcal{J}^{\alpha\beta,\mu}_{ii,k}$ and $\mathcal{J}^{\alpha\beta,\mu\nu}_{ij,ii}$, may be contributed by the terms determined by single-site scattering matrix corrections, which are not only linear with respect to $\delta\hat{e}^\alpha_i$ and $u^\mu_i$ [see Eqs. (6) and (12)], but also quadratic, i.e., $\delta\hat{e}^\alpha_i \delta\hat{e}^\beta_i \underline{T}^{(2)\alpha\beta}_i$ (see for instance [15]) and $u^\mu_i u^\nu_i \underline{\mathcal{U}}^{(2)\mu\nu}_i$ (see Appendix C), respectively.

In order to check the numerical results for three- and four-site SLC parameters, $\mathcal{J}_{ij,k}$, $\mathcal{J}_{ij,kl}$, obtained using the expressions in Eqs. (8) and (9), auxiliary calculations have been performed delivering information about the changes of the exchange coupling parameters occurring due to a displacement of one atom from its equilibrium position. For this purpose, the two-site SSC parameters $J^{\alpha\beta}_{ij}(u^\mu_i)$ have been calculated for a cluster composed of 27 atoms, embedded into a bcc Fe lattice (see Ref. [63]), with the central atom $i$ displaced by $u^\mu_i$ along the $x$ direction, i.e., $\vec{u}_k||\hat{x}$. Taking first- and second-order derivatives of $J^{\alpha\beta}_{ij}(u^\mu_i)$ with respect to $u^\mu_i$ (assuming $\mu = x$) in the limit of $u^\mu_i = 0$ obviously allows a direct comparison to $\mathcal{J}^{\alpha\beta,\mu}_{ij,i}$ and $\mathcal{J}^{\alpha\beta,\mu\mu}_{ij,ii}$. Alternatively, one may multiply $\mathcal{J}^{\alpha\beta,\mu}_{ij,i}$

with $u_i^\mu$ and compare this with $J_{ij}^{\alpha\beta}(u_i^\mu)$ for varying $u_i^\mu$ (also assuming $\mu = x$). Note that all these calculations are performed for a ferromagnetic (FM) reference system with its magnetization $\vec{M}$ along the $z$ axis, i.e., $\vec{M}||\hat{z}$. The corresponding diagonal $\alpha = x$, $\beta = x$ and off-diagonal, $\alpha = x$, $\beta = y$ tensor elements in spin subspace, seen as a function of the displacement $u_i^x$, are compared in Figs. 1(a) and 1(b), respectively. For the diagonal terms shown in Fig. 1(a) one can see two groups of data belonging to atoms $i = 1$–$4$ and $i = 5$–$8$, respectively [see Fig. 1(c) that have opposite sign. Obviously, a rather good agreement between the data for $J_{ij}^{xx}(u_i^x)$ and $\mathcal{J}_{ij,i}^{xx,x} \cdot u_i^x$ is found for a small amplitude of the displacement. The same applies also for the off-diagonal terms shown in Fig. 1(b). When the displacement amplitude increases, the diagonal elements $J_{ij}^{xx}(u_j^x)$ deviate from the linear dependence on the displacement, increasingly with its amplitude. On the other hand, the off-diagonal terms show an additional splitting up and down away from a linear variation, both for the curves showing positive and negative sign. This can be attributed to the impact of higher-order terms with respect to the displacement. To check this, additional calculations have been performed accounting for second-order contributions to the exchange coupling tensor, quadratic with respect to the displacements giving access to the combination $\mathcal{J}_{ij,i}^{\alpha\beta,x} \cdot u_i^x + \mathcal{J}_{ij,ii}^{\alpha\beta,xx} \cdot u_i^x u_i^x$. The second term is calculated using the expression for the SLC tensor elements given by Eq. (9), assuming $k = i$ and $l = i$. Note, however, that in this case (i.e., $k = i$ and $l = i$) an additional second-order contribution $\mathcal{J}_{ij,ii}^{(2)\alpha\beta,\mu\nu}$ has to be taken into account, represented by the expression

$$\mathcal{J}_{ij,ii}^{(2)\alpha\beta,\mu\nu} = -\frac{1}{2\pi}\text{Im Tr} \int^{E_F} dE\left[\underline{T}_i^\alpha \underline{\tau}_{ij} \underline{T}_j^\beta \underline{\tau}_{ji} \underline{\mathcal{U}}_i^{(2)\mu\nu} \underline{\tau}_{ii} \right.$$
$$\left. + \underline{T}_i^\alpha \underline{\tau}_{ii} \underline{\mathcal{U}}_i^{(2)\mu\nu} \underline{\tau}_{ij} \underline{T}_j^\beta \underline{\tau}_{ji}\right], \quad (10)$$

where $\underline{\mathcal{U}}_i^{(2)\mu\nu}$ stems from the second-order derivative of the distorted matrix $\underline{m}_k$ with respect to the displacement (see Appendix C), which includes the following two contributions:

$$\Delta_{\mu\nu}^{2,u}\underline{m}_i = u_i^\mu u_i^\nu \left(\underline{\mathcal{U}}_i^{(2a)\mu\nu} + \underline{\mathcal{U}}_i^{(2b)\mu\nu}\right) \quad (11)$$

with

$$\underline{\mathcal{U}}_i^{(2a)\mu\nu} = -\left(\underline{U}^\mu(\hat{u}_i)\underline{m}_i\underline{U}^\nu(\hat{u}_i) + \underline{U}^\mu(\hat{u}_i)\underline{m}_i\underline{U}^\nu(\hat{u}_i)\right),$$
$$\underline{\mathcal{U}}_i^{(2b)\mu\nu} = \left(\underline{\bar{U}}^{(2)\mu\nu}(\hat{u}_i)\underline{m}_i + \underline{m}_i \underline{\bar{U}}^{(2)\mu\nu}(\hat{u}_i)\right). \quad (12)$$

The dependencies of the terms $\mathcal{J}_{ij,i}^{xx,x} \cdot u_i^x + \mathcal{J}_{ij,ii}^{xx,xx} \cdot u_i^x u_i^x$ and $\mathcal{J}_{ij,i}^{xy,x} \cdot u_i^x + \mathcal{J}_{ij,ii}^{xy,xx} \cdot u_i^x u_i^x$ on the displacement are shown in Figs. 1(a) and 1(b), respectively, by dashed-dotted line, demonstrating their good agreement with $\Delta J_{ij}^{xx}(u_i^x)$ and $\Delta J_{ij}^{xy}(u_i^x)$, respectively, calculated for an embedded cluster with a displaced atom in the center. In addition, the dependence of the $\Delta J_{ij}^{xx}(u_i^x)$ parameter on the position of atom $j$ is determined by corresponding dependencies of the three-site and four-site parameters $\mathcal{J}_{ij,i}^{xy,x}$ and $\mathcal{J}_{ij,ii}^{xy,xx}$ presented in Table I.

The different sign of the parameters $\mathcal{J}_{ij,i}^{xy,x}$ row (a) in the Table 1 indicates a different slope for the two linear branches $\mathcal{J}_{ij,i}^{xy,x} \cdot u_i^x$ that can be observed for two groups of atoms $j$ in Fig. 1(b), positive for $j = \{1, 2, 5, 6\}$ and negative for $j = \{3, 4, 7, 8\}$. The parameters $\mathcal{J}_{ij,ii}^{xy,xx}$ given in row (b) of
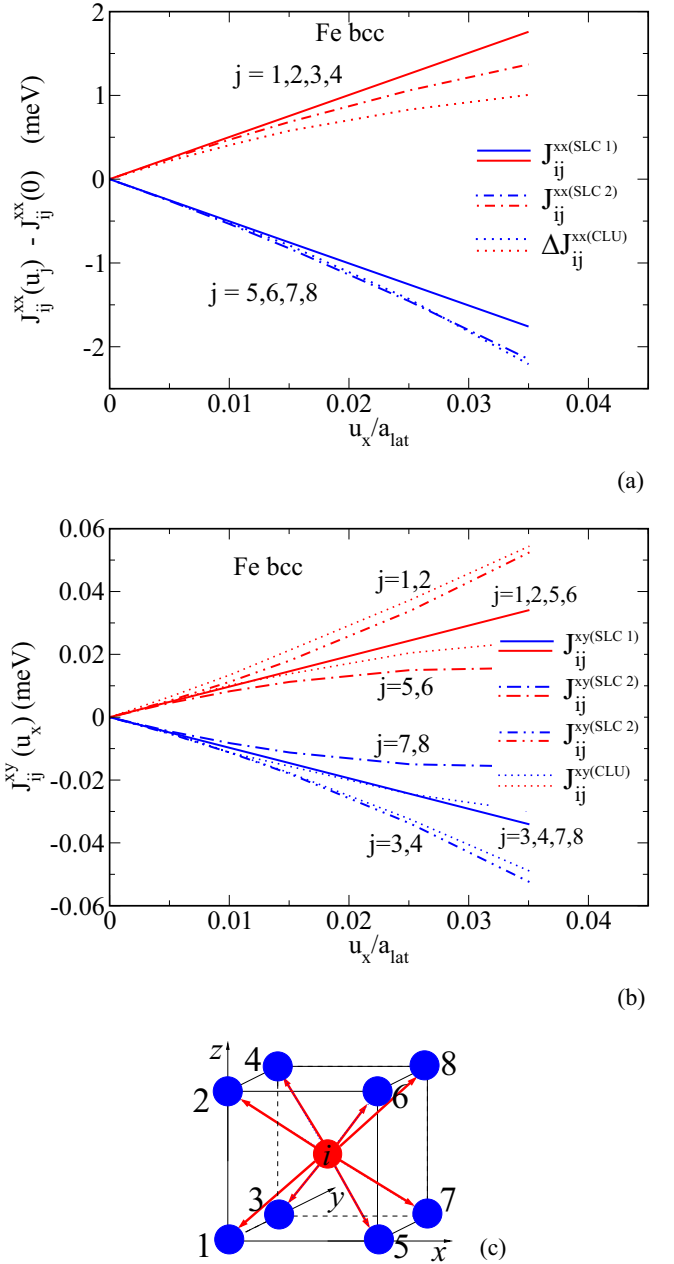


(a)



(b)



(c)

FIG. 1. The corrections of the diagonal (a) and off-diagonal (b) exchange parameters, $\Delta J_{ij}^{xx}(u_i^x)$ and $\Delta J_{ij}^{xy}(u_i^x)$ (dotted lines), respectively due to an atomic displacement $u_i^x$ of atom $i$ along the $x$ axis, calculated for bcc Fe. The results are compared with those based on the SLC parameters multiplied by the corresponding displacement $J_{ij}^{xx(SLC1)} = \mathcal{J}_{ij,i}^{xx,x} \cdot u_i^x$ and $J_{ij}^{xy(SLC1)} = \mathcal{J}_{ij,i}^{xy,x} \cdot u_i^x$ (solid lines), as well as $J_{ij}^{xx(SLC2)} = \mathcal{J}_{ij,i}^{xx,x} \cdot u_i^x + \mathcal{J}_{ij,ii}^{xx,xx} \cdot u_i^x u_i^x$ (a) and $J_{ij}^{xy(SLC2)} = \mathcal{J}_{ij,i}^{xy,x} \cdot u_i^x + \mathcal{J}_{ij,ii}^{xy,xx} \cdot u_i^x u_i^x$ (b) (dashed-dotted lines) plotted as a function of displacement amplitude. (c) Labeling of the nearest-neighbor atoms for a bcc lattice: A displaced atom $i$ at the center is surrounded by atoms $j$ with $\vec{R}_{ij} = \vec{R}_j - \vec{R}_i$.

Table I characterize the curvature of the function $\mathcal{J}_{ij,ii}^{xy,xx} \cdot u_i^x u_i^x$ quadratic with respect to the displacement. Within the first group of neighbors, the curvature is positive for $j = 1, 2$ and negative for $j = 5, 6$, while within the second group it is positive for $j = 7, 8$ and negative for $j = 2, 4$. As a

TABLE I. The nearest-neighbor three-site $\mathcal{J}_{ij,i}^{xy,x}$ (a) and four-site $\mathcal{J}_{ij,ii}^{xy,xx}$ (b) SLC parameters [meV/a.u. and meV/(a.u.)$^2$ units, respectively]. The results are given for the shifted atom $i$ at the center and the nearest-neighbor sites $j$ [see Fig. 1(c).

| $i$ | 1 | 2 | 3 | 4 | 5 | 6 | 7 | 8 |
|---|---|---|---|---|---|---|---|---|
| a | 0.182 | 0.182 | –0.182 | –0.182 | 0.182 | 0.182 | –0.182 | –0.182 |
| b | 0.506 | 0.506 | –0.506 | –0.506 | –0.506 | –0.506 | 0.506 | 0.506 |

consequence, the quadratic contribution results in a splitting of the linear branches in line with the results for $\mathcal{J}_{ij}^{xy}(u_i^x)$ obtained from self-consistent calculations for embedded clusters with a displaced atom $i$.

The antisymmetric part of the off-diagonal three-site SLC tensor elements can be seen as the Dzyaloshinskii-Moriya interaction $D_{ij}^z$ induced by the symmetry-breaking displacement of atom $k$, i.e., $\mathcal{D}_{ij,k}^{z,\mu} = \frac{1}{2}(\mathcal{J}_{ij,k}^{xy,\mu} - \mathcal{J}_{ij,k}^{yx,\mu})$, that occurs despite the conventional DMI represented by $D_{ij}^\alpha$ vanishes for the nondistorted bcc Fe lattice due to inversion symmetry. The same applies also for the four-site SLC parameters $\mathcal{D}_{ij,kl}^{z,\mu\nu}$.

For illustration, the three-site and four-site SLC parameters characterizing the spin-spin coupling between the nondisplaced atom $i$ and displaced atom $j$ have been calculated for FM-ordered bcc Fe. Figure 2 represents the diagonal $\mathcal{J}_{ij,j}^{xx,\mu}$ and DMI-like $\mathcal{D}_{ij,j}^{z,\mu}$ SLC parameters plotted as a function of the interatomic distance $R_{ij}$, for different directions $u_x$, $u_y$, $u_z$ of the displacement. Both Figs. 2(a) and 2(b) look symmetric with respect to a sign inversion of the SLC parameters as a consequence of the above mentioned spitting of the parameters into two groups with opposite sign. Of course, these groups behave differently depending on the direction of the displacement $\vec{u}_j$. Moreover, for the DMI-like SLC parameters, one can see different magnitudes of the $\mathcal{D}_{ij,j}^{z,z}$ parameters (i.e., for $\vec{u}_j$ parallel to the DMI vector) when compared to $\mathcal{D}_{ij,j}^{z,x}$ and $\mathcal{D}_{ij,j}^{z,y}$ with the displacements perpendicular to the DMI vector.

The SLC tensor with the elements $\mathcal{J}_{ij,k}^{\alpha\alpha,\mu}$, multiplied by spin tiltings $\delta\hat{e}_{i(j)}$ on sites $i$ and $j$ represents a force acting on the atom on site $k$. These forces can lead to a structure instability induced by magnetic order in a system as mentioned in the introduction.

Let us discuss the forces $\vec{\mathcal{F}}$ generated due to the symmetric diagonal $\mathcal{J}_{ij,j}^{\mathrm{dia-s},\mu} = \frac{1}{2}(\mathcal{J}_{ij,j}^{xx,\mu} + \mathcal{J}_{ij,j}^{yy,\mu})$ and DMI-like $\mathcal{D}_{ij,j}^{\alpha,\mu}$ spin-lattice interactions, as shown in the left panels of Figs. 3(a) and 3(b), respectively. Considering FM bcc Fe with the magnetization direction along the $z$ axis, the corresponding forces generated due to a rotation of the spin moments on sites $i$ and $j$, $\hat{e}_{i(j)} \approx \hat{z} + \delta\hat{e}_{i(j)}^x$ have the components $-\mathcal{J}_{ij,j}^{\mathrm{dia-s},\mu}\delta e_i^x \delta e_j^x$ and $-\mathcal{D}_{ij,j}^{y,\mu}(\hat{e}_i \times \hat{e}_j)_y = -\mathcal{D}_{ij,j}^{y,\mu}(\hat{e}_i^z \delta\hat{e}_j^x - \hat{e}_j^z \delta\hat{e}_i^x)$, respectively. In Fig. 3 the arrows show the quantities $\vec{f}_j = -\sum_\mu \mathcal{J}_{ij,j}^{\mathrm{dia-s},\mu}\hat{n}_\mu$ (a) and $\vec{f}_j = -\sum_\mu \mathcal{D}_{ij,j}^{y,\mu}\hat{n}_\mu$ (b) (with the unit vectors $\hat{n}_x = \hat{x}$, $\hat{n}_y = \hat{y}$, $\hat{n}_z = \hat{z}$), which determine corresponding forces $\vec{F}_j$ on the atoms at site $j$, arising due to spin tiltings within the $x - z$ plane. The results are presented for two atomic shells around atom $i$. As one can see, the forces originated from the diagonal symmetric elements of the SLC tensor are directed along the
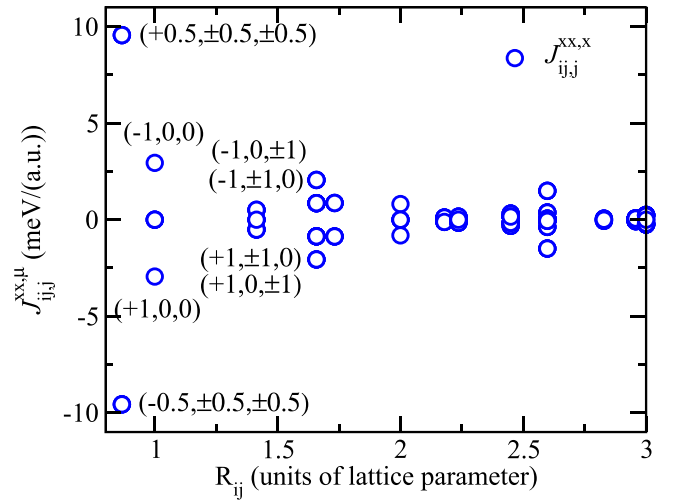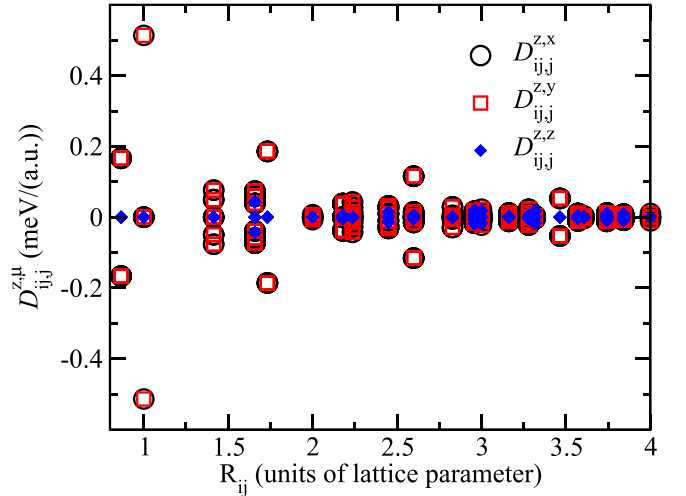


FIG. 2. (a) Diagonal SLC parameters $\mathcal{J}_{ij,j}^{xx,x}$ for bcc Fe as a function of the interatomic distance $R_{ij}$. A similar behavior was obtained for $\mathcal{J}_{ij,j}^{xx,y}$ and $\mathcal{J}_{ij,j}^{xx,z}$. In case of $\vec{R}_{ij} \perp \vec{u}$ all SLC parameters are zero. The vectors next to the data points give the relative position $\vec{R}_{ij}$ of the sites $j$ for the first three atomic shells around the central site $i$. (b) Corresponding results for the DMI-like parameters $\mathcal{D}_{ij,j}^{z,\mu}$.

lines connecting the interacting atoms. This may lead to a lattice distortion being the result of a competition with the elastic forces between the atoms. On the other hand, as one can see in Fig. 3(b), the forces originating from the antisymmetric elements of the SLC tensor, i.e., the DMI-like SLC parameters, are perpendicular to the lines connecting the interacting atoms, creating a mechanical torque on the lattice dependent on the magnetic configurations, that can lead to an angular momentum transfer upon the magnon-phonon scattering events [53,64,65].

Figures 4 and 5 represent the four-site SLC parameters, $\mathcal{J}_{ij,ij}^{\mathrm{dia-s},\mu\nu} = \frac{1}{2}\sum_k(\mathcal{J}_{ij,ij}^{xx,\mu\nu} + \mathcal{J}_{ij,ij}^{yy,\mu\nu})$ and $\mathcal{D}_{ij,ij}^{z,\mu\nu}$, respectively, plotted as a function of the interatomic distance $R_{ij}$. In this case both atoms $i$ and $j$ are assumed to be displaced from the equilibrium. One can see a dominating nearest-neighbor
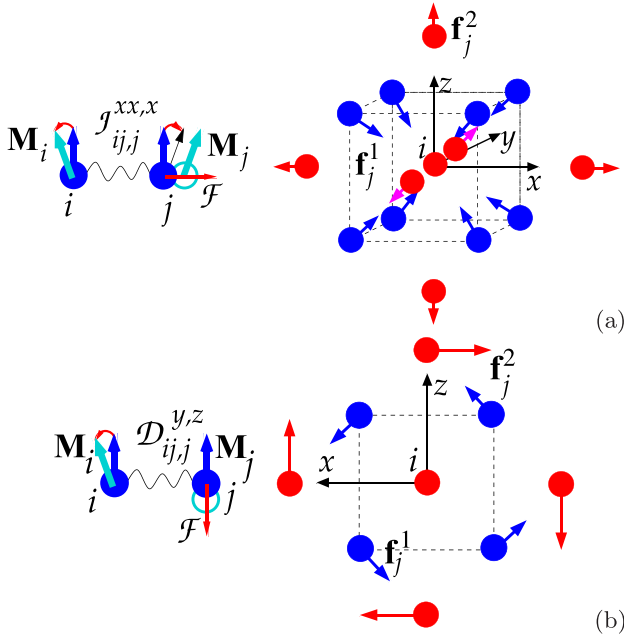
FIG. 3. The quantities $\vec{f}_j = -\sum_\mu \mathcal{J}_{ij,j}^{\text{dia}-s,\mu} \hat{n}_\mu$ (a) and $\vec{f}_j = -\sum_\mu \mathcal{D}_{ij,j}^{y,\mu} \hat{n}_\mu$ (b) ($\hat{n}_x = \hat{x}$, $\hat{n}_y = \hat{y}$, $\hat{n}_z = \hat{z}$) associated with the symmetric diagonal and DMI-like SLC, respectively, characterizing the forces on atoms $j$ induced by spin tilting on site $i$ via the spin-lattice coupling in bcc Fe with the magnetization along $z$ axis. The left panel shows schematically the SLC-mediated force $\vec{\mathcal{F}}$ on atom $j$ (red arrow) induced by tilting of the spin moments on sites $i$ and $j$ (shown in light blue color), and vice versa, the spin tiltings induced due to the displacements of the atom on site $j$ (light blue circle). In the right panel, the arrows show the directions of the forces for the first and second atomic shells, blue and red, respectively. In the case (a) the forces are directed along the lines connecting the interacting atoms, with $\vec{f}_j = 9.56(\pm1, \pm1, \pm1)$ for the first shell and $\vec{f}_j = -2.9(0, 0, \pm1)$, $\vec{f}_j = -2.9(0, \pm1, 0)$, $\vec{f}_j = -2.9(\pm1, 0, 0)$ for the second shell. In the case (b) the forces are perpendicular to the lines connecting the interacting atoms, with $\vec{f}_j^1 = 0.16(\pm1, 0, \pm1)$ for the first shell and $\vec{f}_j^2 = 0.5(0, 0, \pm1)$, $\vec{f}_j^2 = 0.5(\pm1, 0, 0)$ for the second shell.

coupling $\mathcal{J}_{ij,ij}^{\text{dia}-s,\mu\nu}$ in the case of $\mu \neq \nu$, while the $\mathcal{J}_{ij,ij}^{\text{dia}-s,\mu\mu}$ coupling has a comparable strength for several neighboring shells. The SOC-driven DMI-like parameters are about two orders of magnitude smaller, and are strongly determined by the local symmetry depending on the directions of the displacements and the direction of the $\vec{\mathcal{D}}_{ij,ij}^{\mu\nu}$ vector. In particular, as is shown in Fig. 5(a), the $\mathcal{D}_{ij,ij}^{z,\mu\nu}$ component is equal to zero for the displacement of atoms $i$ and $j$ along the same direction.

At finite temperature the exchange parameters are modified not only by a single but all thermally excited phonons. This problem was considered in the literature by various groups [18,44,45]. In particular, the Debye model that provides a simple connection between the thermal average of the squared displacement $\langle u^2 \rangle_T^D$ and the lattice temperature $T$ has been taken as a basis to account for thermal vibrations. Using this relation, the dependence of the exchange parameters $J_{ij}$ on the temperature $T$ has been determined
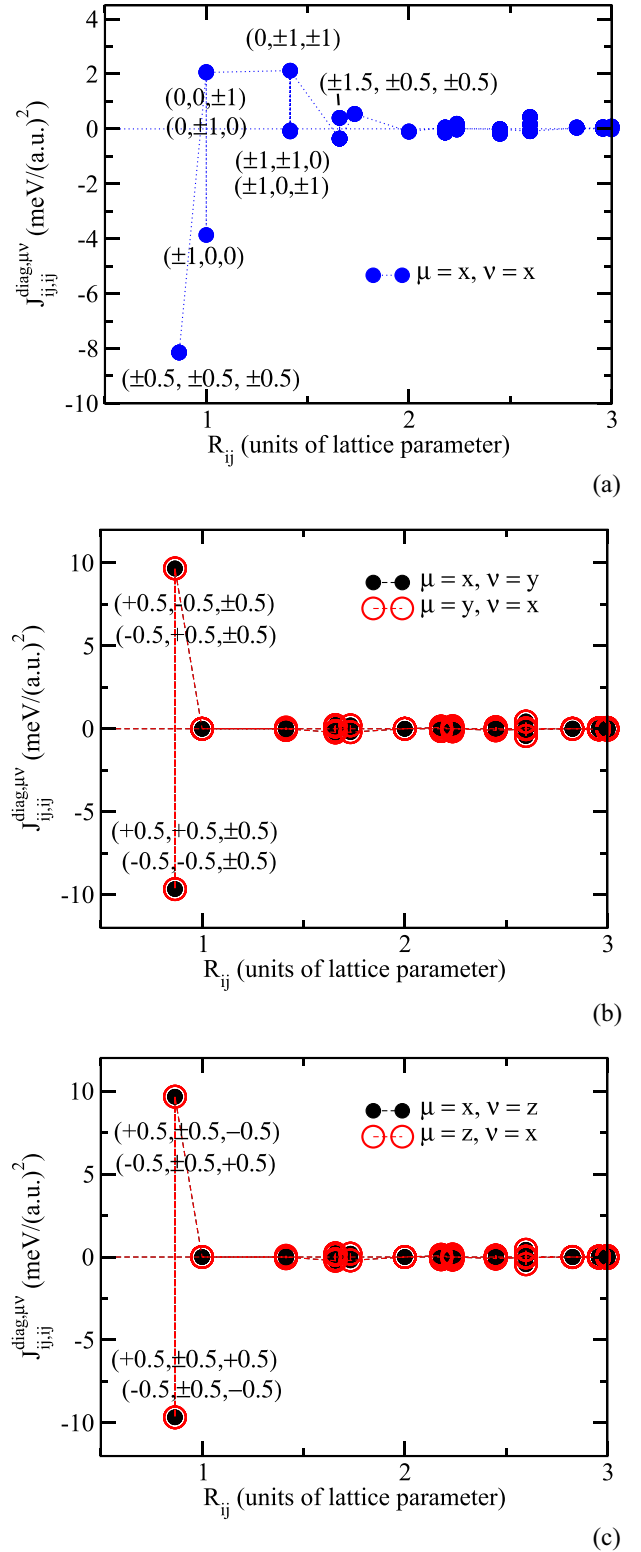


FIG. 4. The SLC parameters $\mathcal{J}_{ij,ij}^{\text{dia}-s,\mu\nu}$, diagonal with respect to spin $\alpha = \beta$ and (a) diagonal with respect to displacement indices $\mu = \nu = x$ [the trend is similar for $\mu = \nu = y(z)$], and off-diagonal with respect to displacement indices, $\mu \neq \nu$, (b) for $\mu = \{x, y\}$ and $\nu = \{x, y\}$ and (c) for $\mu = \{x, z\}$ and $\nu = \{x, z\}$, represented as a function of interatomic distance $R_{ij}$. The vectors next to the data points give the relative position $\vec{R}_{ij}$ of the sites $j$ for the first three atomic shells around the central site $i$.
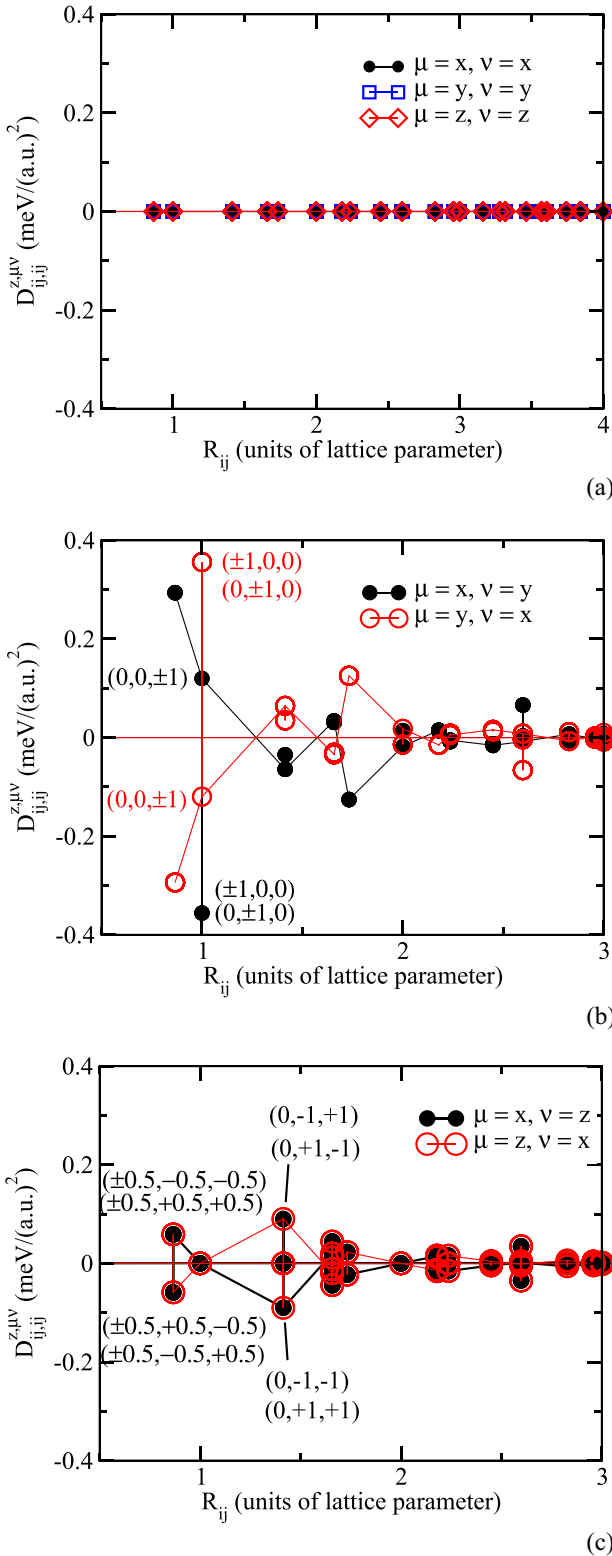
(a)



(b)



(c)

FIG. 5. The DMI-like SLC parameters $\mathcal{D}_{ij,ij}^{z,\mu\nu}$ diagonal with respect to displacement indices $\mu = \nu$ (a), and off-diagonal with respect to displacement indices, $\mu \neq \nu$, (b) for $\mu = \{x, y\}$ and $\nu = \{x, y\}$ and (c) for $\mu = \{x, z\}$ and $\nu = \{x, z\}$, represented as a function of interatomic distance $R_{ij}$. The parameters $\mathcal{D}_{ij,ij}^{z,xy}$ and $\mathcal{D}_{ij,ij}^{z,yx}$ in (b) have for the same $\vec{R}_{ij}$ the same magnitude but opposite sign. The vectors next to the data points give the relative position $\vec{R}_{ij}$ of the sites $j$ for the first three atomic shells around the central site $i$.
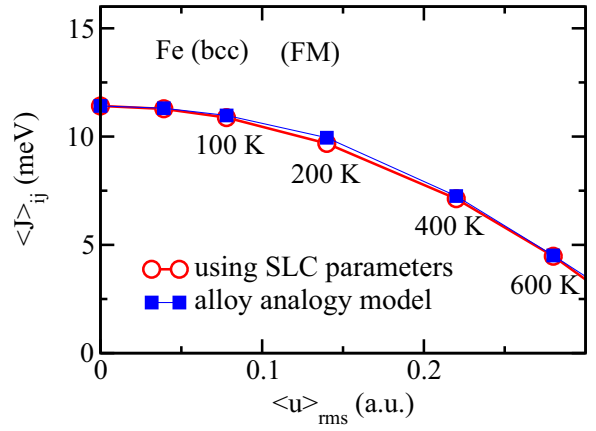


FIG. 6. The dependence of the nearest-neighbor exchange coupling parameters $\langle J_{ij} \rangle_T$ of bcc Fe on the root-mean-square thermal displacement $\sqrt{\langle u^2 \rangle_T^D}$ of the atoms. Corresponding temperatures are attached to some data points. Open symbols represent the results based on the SLC parameters using Eq. (14) while full squares correspond to results obtained via the alloy-analogy model [66].

self-consistently on the basis of the so-called alloy analogy model [66]. As the SLC parameters $\mathcal{J}_{ij,k}^{diag,\mu}$ and $\mathcal{J}_{ij,kl}^{diag,\mu\nu}$ characterize the corrections of the corresponding parameters $J_{ij}$ caused by displacements $u_k^\mu$, one can estimate the temperature dependent $\langle J_{ij} \rangle_T$ by averaging over all lattice excitations corresponding to a given temperature $T$. This can be expressed as follows:

$$\langle J_{ij} \rangle_T = J_{ij}^0 + \sum_{k,\mu} \mathcal{J}_{ij,k}^{diag,\mu} \langle u_k^\mu \rangle_T + \sum_{kl,\mu\nu} \mathcal{J}_{ij,kl}^{diag,\mu\nu} \langle u_k^\mu u_l^\nu \rangle_T + \dots .$$

(13)

As the average $\langle u_k^\mu \rangle_T$ of the linear term vanishes, the second-order SLC parameters give rise to the lowest-order contribution to the temperature dependence of the exchange parameters. Accounting only for the displacements of the interacting atoms and using $\langle u_k^\mu u_l^\nu \rangle_T = \delta_{\mu\nu} \langle u_k^\mu u_l^\mu \rangle_T$ we can approximate the thermal average of the parameters as follows:

$$\langle J_{ij} \rangle_T = J_{ij}^0 + \sum_\mu \mathcal{J}_{ij,ij}^{diag,\mu\nu} \langle u_i^\mu u_j^\mu \rangle_T + \sum_\mu \mathcal{J}_{ij,ii}^{diag,\mu\nu} \langle u_i^\mu u_i^\mu \rangle_T$$
$$+ \sum_\mu \mathcal{J}_{ij,jj}^{diag,\mu\nu} \langle u_j^\mu u_j^\mu \rangle_T .$$

(14)

To evaluate this expression we use for the averaged displacements the approximation $\langle u_i^\mu u_j^\mu \rangle_T = \langle u^2 \rangle_T^D$ with $\langle u^2 \rangle_T^D$ given by the Debye model. The values for $\langle J_{ij} \rangle_T$ obtained this way for bcc Fe are compared in Fig. 6 with corresponding results calculated on the basis of the alloy analogy model [66]. One can see that in this particular case the contribution due to displacements of the interacting atoms are dominating, while in general one might have to account also for contributions due to the displacements of all surrounding atoms $l$ and $k$ different from $i$ and $j$.

## III. SITE-DIAGONAL SPIN-LATTICE COUPLING PARAMETERS

### A. Phenomenology: MCA-like spin-lattice Hamiltonian

In addition to the interatomic spin-lattice interaction, the SLC Hamiltonian in Eq. (1) includes also a contribution to be seen as a counterpart to the magnetic anisotropy in the spin Hamiltonian

$$\mathcal{H}_{MA} = \sum_{i,\alpha,\beta} K_i^{\alpha\beta} e_i^\alpha e_i^\beta + \sum_{i,\alpha,\beta,\gamma,\delta} K_i^{\alpha\beta\gamma\delta} e_i^\alpha e_i^\beta e_i^\gamma e_i^\delta + \ldots \quad (15)$$

with the nonvanishing terms determined by the symmetry of the crystal. The corresponding MCA-like terms in the spin-lattice Hamiltonian in Eq. (1) characterize contributions to the magnetic anisotropy at any site, arising due to a displacement of surrounding atoms, breaking the local symmetry of the crystal. Furthermore, these parameters give rise to a dominating contribution to the spin-phonon interactions for some materials as it was discussed for instance in Refs. [67–69].

The induced magnetic anisotropy energy in the Hamiltonian is characterized by the anisotropy constants, which may include different contributions discussed in the literature, controlled by dipole-dipole interactions and the spin-orbit coupling (SOC) [70]. When comparing the dipole-dipole contribution to the anisotropy and magnetostriction observed experimentally, Lee [70] points out that it represents only a small part of the observed values. This led him to the conclusion that the magnetoelastic constants are primarily determined by SOC.

Therefore we focus here on the SOC-driven spin-lattice coupling responsible for the local magnetic anisotropy induced by a lattice distortion breaking the local symmetry in the system. Dealing with the atomistic spin-lattice Hamiltonian keeping the lowest-order terms linear with respect to the atomic displacements according to the expression

$$\mathcal{H}_{\text{me-MA}} = \sum_{i,k} \sum_\mu \left( \mathcal{K}_{i,k}^{xx,\mu} u_k^\mu e_i^x e_i^x + \mathcal{K}_{i,k}^{yy,\mu} u_k^\mu e_i^y e_i^y \right.$$
$$+ \mathcal{K}_{i,k}^{zz,\mu} u_k^\mu e_i^z e_i^z + \mathcal{K}_{i,k}^{xy,\mu} u_k^\mu e_i^x e_i^y$$
$$\left. + \mathcal{K}_{i,k}^{xz,\mu} u_k^\mu e_i^x e_i^z + \mathcal{K}_{i,k}^{yz,\mu} u_k^\mu e_i^y e_i^z \right), \quad (16)$$

we will discuss below an approach providing the basis for calculations of the SLC parameters of the Hamiltonian in Eq. (1) on a first-principles level. Some contributions to the expression in Eq. (16) have been discussed already [53], which correspond to the site-diagonal SLC tensor $\underline{\mathcal{J}}_{ii,k}$, both, diagonal, e.g., $\mathcal{J}_{ii,k}^{\text{dia-a},\mu} = \frac{1}{2}(\mathcal{J}_{ii,k}^{\alpha\alpha,\mu} - \mathcal{J}_{ii,k}^{\beta\beta,\mu})$ and off-diagonal, e.g., $\mathcal{J}_{ii,k}^{\text{off-s},\mu} = \frac{1}{2}(\mathcal{J}_{ii,k}^{xy,\mu} + \mathcal{J}_{ii,k}^{yx,\mu})$ terms. However, there are further contributions, which have to be taken into account, similar to those discussed in Ref. [15] considering various contributions to the MCA. In particular, one should mention the so-called nonlocal contribution associated with the anisotropy of the three-site SLC $\mathcal{J}_{ij,k}^{\text{dia-a},\mu} = \frac{1}{2}(\mathcal{J}_{ij,k}^{\alpha\alpha,\mu} - \mathcal{J}_{ij,k}^{\beta\beta,\mu})$, similar to the so-called nonlocal contribution $\frac{1}{2}(\mathcal{J}_{ij}^{\alpha\alpha} - \mathcal{J}_{ij}^{\beta\beta})$ to the uniaxial magnetic anisotropy discussed in Ref. [15].

As an alternative, we are going to use a scheme based on the magnetic torque [56] (see Appendix D), to get access

to the parameters of the MA-SLC Hamiltonian in Eq. (16). Focusing on the terms $\mathcal{K}_{i,k}^{\alpha z,\mu} e_i^\alpha e_i^z u_k^\mu$, the SLC parameters are directly connected to the effective field determined as

$$\vec{H}_{i,\text{eff-SLC}\alpha z} = -\frac{\partial}{\partial e_i^\alpha} \mathcal{H}_{\text{me-MA}}|_{\theta=0}, \quad (17)$$

and can be calculated as follows:

$$\mathcal{K}_{i,k}^{\alpha z,\mu} e_i^z = \frac{\partial}{\partial^2 e_i^\alpha \partial u_k^\mu} \mathcal{H}_{\text{me-MA}}|_{\theta=0}$$
$$= -\frac{\partial}{\partial u_k^\mu} \vec{H}_{i,\text{eff-SLC}\alpha z}. \quad (18)$$

For the FM reference state with the equilibrium magnetization direction along the $z$ axis, one has $e^x \approx \theta$, $e^y \approx \theta$ and $e^z \approx 1 - \frac{1}{2}\theta^2 \approx 1$, assuming a small spin tilting $\theta$ from the equilibrium. This allows to redefine for the sake of convenience the SLC parameters as follows: $\mathcal{K}_{i,k}^{\alpha z,\mu} e_i^z \to \tilde{\mathcal{K}}_{i,k}^{\alpha z,\mu}$ [39,41,71], keeping in mind that the newly defined parameters are antisymmetric with respect to time reversal and their original form should be used in the dynamical equations. The corresponding SLC parameters can be calculated via the first derivative with respect to the spin direction, i.e.,

$$\tilde{\mathcal{K}}_{i,k}^{\alpha z,\mu} = \frac{\partial}{\partial e_i^\alpha \partial u_k^\mu} \mathcal{H}_{\text{me-MA}}|_{\theta=0} = \frac{\partial}{\partial e_i^\alpha \partial u_k^\mu} F|_{\theta=0}. \quad (19)$$

### B. Torque: First-principles approach

As a starting point we use the ferromagnetic (FM) state as a reference state and neglect for the moment all temperature effects, i.e., assume $T = 0$ K. Instead of using the Lloyd formula, we represent the change of free energy $\Delta F$ in terms of the Green's function $G_0(E)$ for the FM reference state, which is modified due to the perturbation. Denoting the corresponding change in the Green's function $\Delta G(E)$ and neglecting temperature effects one can write the change of the total energy,

$$\Delta F = -\frac{1}{\pi} \text{Im Tr} \int^{E_F} dE \, (E - E_F) \Delta G(E), \quad (20)$$

where $E_F$ is the Fermi energy. Assuming that the perturbations are small, the induced change of the Green's function can be represented by the following perturbative expansion:

$$\Delta G(E) = G_0(E) \Delta V_m G_0(E)$$
$$+ G_0(E) \Delta V_m G_0(E) \Delta V_m G_0(E) + \ldots$$
$$+ G_0(E) \Delta V_m G_0(E) \Delta V_u G_0(E) + \ldots, \quad (21)$$

where $\Delta V_m$ describes a perturbation due to the spin tilting, and $\Delta V_u$ is a perturbation due to a lattice distortion in the system. It should be noted that we omit in Eq. (21) the terms determined by the atomic displacements only, as well as all higher-order terms. Below we will focus on the first and third terms in this expression, as they give rise to the magnetic torque for the nondistorted lattice and account for its distortion, respectively.

Substituting Eq. (21) into Eq. (20) and using the sum rule $\frac{dG}{dE} = -GG$ for the Green's function, one obtains an expression for the total energy change associated with the

perturbations,

$$\Delta F = \frac{1}{\pi} \mathrm{Im} \, \mathrm{Tr} \int^{E_F} dE \, (E - E_F) \, \Delta V_m \frac{dG_0(E)}{dE}$$
$$+ \frac{1}{\pi} \mathrm{Im} \, \mathrm{Tr} \int^{E_F} dE \, (E - E_F) \Delta V_m G_0(E) \Delta V_u \frac{dG_0(E)}{dE} \, .$$
(22)

We keep here only the first- and second-order terms that give access to the magnetic torque for the crystal, without and with a lattice distortion, respectively.

By performing an integration by parts for the second equation in Eq. (22) and taking into account that $(E - E_F) \, \Delta V_m \, G_0(E)|_{E=E_F} = 0$ and $(E - E_F) \, \Delta V_m \, G_0(E) \Delta V_u \, G_0(E)|_{E=E_F} = 0$, the free energy change $\Delta F$ is given by

$$\Delta F = -\frac{1}{\pi} \mathrm{Im} \, \mathrm{Tr} \int^{E_F} dE \, \Delta V \, G_0(E)$$
$$- \frac{1}{\pi} \mathrm{Im} \, \mathrm{Tr} \int^{E_F} dE \, \Delta V_m G_0(E) \Delta V_u G_0(E) \quad (23)$$
$$= F^{(1)} + F^{(2)} \, . \quad (24)$$

Representing the Green's function in terms of the multiple scattering formalism [63], Eq. (24) leads to the expression

$$\Delta F = -\frac{1}{\pi} \mathrm{Im} \, \mathrm{Tr} \int^{E_F} dE \, \langle \Delta \underline{V}_m \rangle \, \underline{\tau}(E)$$
$$- \frac{1}{\pi} \mathrm{Im} \, \mathrm{Tr} \int^{E_F} dE \, \langle \Delta \underline{V}_m \rangle \underline{\tau}(E) \langle \Delta \underline{V}_u \rangle \underline{\tau}(E) \, . \quad (25)$$

Using for the matrix elements of perturbation $\langle \Delta \underline{V}_m \rangle$ and $\langle \Delta \underline{V}_u \rangle$ the expressions (see Appendix C)

$$\langle \Delta \underline{V}_m \rangle = \sum_\alpha \delta \hat{e}_i^\alpha \, \underline{T}_i^\alpha, \quad (26)$$

$$\langle \Delta \underline{V}_u \rangle = \sum_\nu u_i^\nu \underline{\mathcal{U}}_i^\nu, \quad (27)$$

and taking the derivatives $\frac{\partial F^{(1)}}{\partial e^\alpha}$ and $\frac{\partial^2 F^{(2)}}{\partial e^\alpha \partial u^\mu}$, one obtains for the magnetic anisotropy constants

$$\tilde{K}_i^{\alpha z} = \frac{\partial \Delta F}{\partial e_i^\alpha}\bigg|_{u=0} = -\frac{1}{\pi} \mathrm{Im} \, \mathrm{Tr} \int^{E_F} dE \, \underline{T}_i^\nu \, \underline{\tau}_{ii}(E) \quad (28)$$

and their counterparts in the spin-lattice Hamiltonian,

$$\tilde{\mathcal{K}}_{i,k}^{\alpha z, \mu} = \frac{\partial^2 \Delta F}{\partial e_i^\alpha \partial u_k^\mu}\bigg|_{u=0}$$
$$= -\frac{1}{\pi} \mathrm{Im} \, \mathrm{Tr} \int^{E_F} dE \, \underline{T}_i^\mu \underline{\tau}_{ik}(E) \underline{\mathcal{U}}_k^\nu \underline{\tau}_{ki}(E) \, . \quad (29)$$

The parameters $\mathcal{K}_{i,k}^{\alpha z, \mu}$ give access either to the torque on a magnetic moment $\vec{\mathcal{T}}_i = \hat{e}_i \times \vec{H}_{\mathrm{eff}}$ caused by the effective field induced by the displacements $u_k^\mu$ of the atoms on sites $k$, i.e.,

$$\vec{H}_{\mathrm{eff},i}^\alpha = -\sum_{k,\mu} \mathcal{K}_{i,k}^{\alpha z, \mu} \hat{e}_i^z u_k^\mu \, , \quad (30)$$

and characterizing the rate of change of spin angular momentum, or to the mechanical torque, e.g., $\vec{\mathfrak{T}}_k^{ph} = \vec{u}_k \times \vec{\mathcal{F}}_k$ created
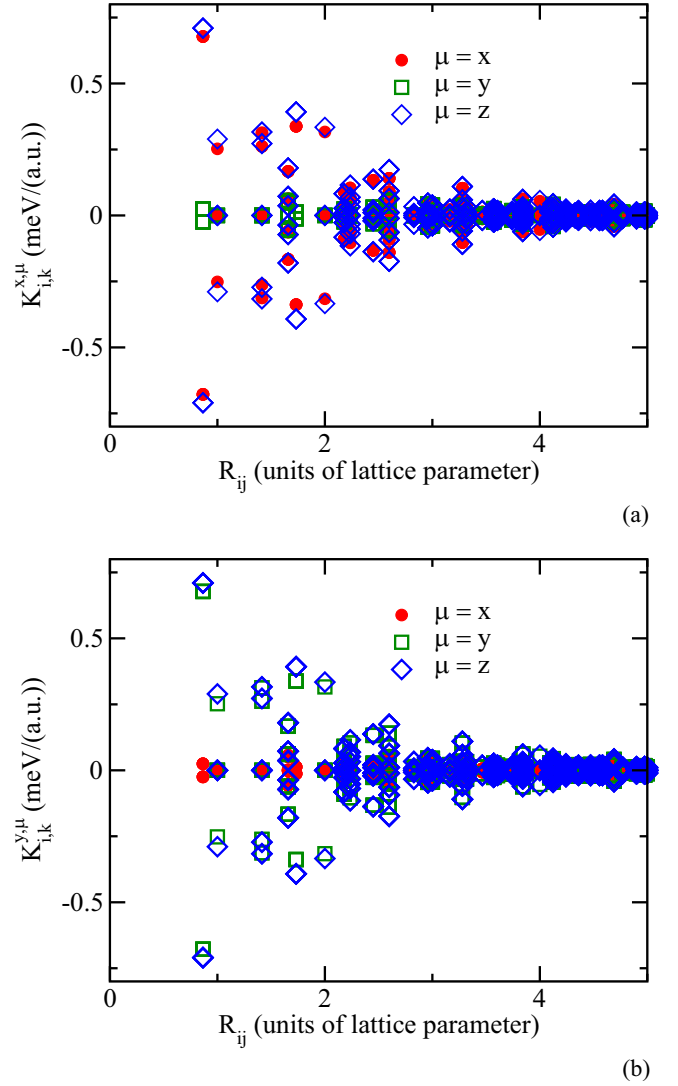


FIG. 7. The parameters $\mathcal{K}_{i,k}^{x,\mu}$ (a) and $\mathcal{K}_{i,k}^{y,\mu}$ (b) calculated for bcc Fe, as a function of the distance $R_{ik}$.

by the forces induced by spin tiltings $\hat{e}_i^\alpha$ on sites $i$, i.e.,

$$\mathcal{F}_k^\mu = -\sum_{i,\alpha} \mathcal{K}_{i,k}^{\alpha z, \mu} \hat{e}_i^\alpha \hat{e}_i^z \, , \quad (31)$$

and contributing to the rate of change of the spin angular momentum of phonons [65]. As an example, the parameters $\mathcal{K}_{i,k}^{\alpha z, \mu}$ and $\mathcal{K}_{i,k}^{yz, \mu}$ calculated for bcc Fe (with the magnetization direction along $z$ axis) are plotted in Fig. 7 as a function of the distance $R_{ik}$, for the three displacements $\mu = x, y, z$. As one can see, their absolute values are much smaller in the case of a displacement perpendicular to the plane of magnetization rotation (i.e., for the $u_y$ component for tilting within the $x - z$ plane and the $u_x$ component for tilting within the $y - z$ planes) when compared to the displacements within the plane.

As it was already pointed out, the displacement of any atom $k$ in the system, obviously, breaks the local symmetry at a neighboring site $i$, creating a corresponding contribution to the magnetic anisotropy and in turn to a corresponding effective field and the torque on the magnetic moment on site $i$. This torque depends on the local symmetry around the displaced
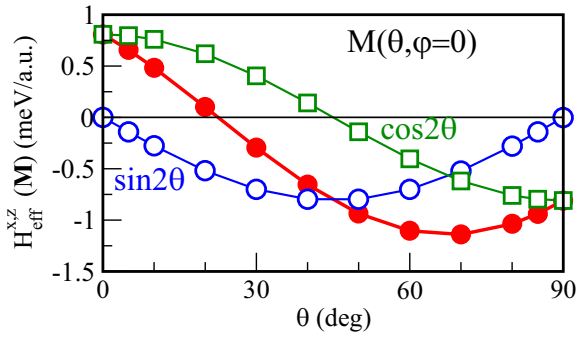
FIG. 8. The dependence of the effective field (closed circles) in bcc Fe on the $\theta$ angle characterizing the direction of the magnetization with respect to $\hat{z}$, in the presence of a single atom displaced along the $\hat{z}$ direction. It is contributed by the terms $\sim(\mathcal{K}_{i,k}^{xx,z} - \mathcal{K}_{i,k}^{zz,z})\sin 2\theta$ (open circles) and $\sim(\mathcal{K}_{i,k}^{xz,z} + \mathcal{K}_{i,k}^{zx,z})\cos 2\theta$ (open squares).

atoms, as well as on the direction of the magnetization with respect to the crystal lattice. Using the phenomenological SLC Hamiltonian, one can see that the contributions to the effective field caused by the displacement $u_k^\mu$, which are associated with different SLC terms in the Hamiltonian, have a different dependence on the magnetization direction.

To demonstrate this dependence, we consider FM-ordered bcc Fe and focus on the term $\sim\mathcal{K}_{i,k}^{xz,\mu}$. In the case of the magnetization oriented along the crystallographic direction [001] and atoms $k$ displaced along the $\hat{z}||(0, 0, 1)$ direction, i.e., $\vec{u} = u_k^z\hat{z}$, the corresponding effective magnetic field induced on site $i$ is equal to $-\mathcal{K}_{i,k}^{xz,z}e_i^z u_k^z$. It determines the induced torque on the magnetic moment on site $i$ responsible for the formation of a noncollinear magnetic structure driven by the lattice distortion. At the same time, the induced effective field due to the terms $\mathcal{K}_{i,k}^{xx,z}e_i^x u_k^z$ and $\mathcal{K}_{i,k}^{yy,z}e_i^y u_k^z$ for such a geometry is equal to zero as $e_i^x \sim \theta = 0$ and $e_i^y \sim \theta = 0$. Rotating the frame of reference together with the magnetization (within the $x - z$ plane by the angle $\theta$), keeping $\hat{\bar{z}}||\hat{m}$, the effective field is calculated via the transformation $\underline{R}_{-\theta}\underline{A}\underline{R}_{-\theta}^{-1}$ with $\underline{A}$ seen as the matrix with the elements $A^{\alpha\beta} \sim \mathcal{K}_{i,k}^{\alpha\beta,z}u_k^z$. As a result, the nonvanishing effective field is given by the expression $H_i^{\bar{x}}(u_k^z) = -\frac{\partial E}{\partial e_i^{\bar{x}}} = -(\mathcal{K}_{i,k}^{\bar{x}z,z} + \mathcal{K}_{i,k}^{z\bar{x},z})e_i^{\bar{z}}u_k^z$, where

$$H_i^{\bar{x}}(u_k^z) = -\frac{1}{2}\big[\big(\mathcal{K}_{i,k}^{xx,z} - \mathcal{K}_{i,k}^{zz,z}\big)\sin 2\theta + \big(\mathcal{K}_{i,k}^{xz,z} + \mathcal{K}_{i,k}^{zx,z}\big)\cos 2\theta\big].$$
(32)

A similar expression can also be found for $\mathcal{K}_{i,k}^{z\bar{x},z}$. Figure 8 represents a particular example of the effective field $H_i^{\bar{x}}(u_k^z)$ on site $i$ [$R_i = (0, 0, 0)$] in bcc Fe, which is created due to a displacement of atom $k$, $R_k = a(0.5, 0.5, 0.5)$, along the crystallographic direction [001], assuming $|u_k^z| = 1$. This field can now be calculated on a first-principles level, using the expression in Eq. (29). The total field is shown by the red solid line, which is a result of two contributions $\sim\sin 2\theta$ and $\cos 2\theta$, shown by blue dashed and green dashed-dotted lines, respectively. In the case of a tetragonal distortion, i.e., a displacement by $u_z$ of the atoms at $a(\pm 0.5, \pm 0.5, 0.5)$ and a displacement by $-u_z$ of the atoms at $a(\pm 0.5, \pm 0.5, -0.5)$, the only nonzero contribution due to the induced effective field is associated with the term $\frac{1}{2}(\mathcal{K}_{i,k}^{xx,z} - \mathcal{K}_{i,k}^{zz,z})$, i.e., $\sim\sin 2\theta$, that
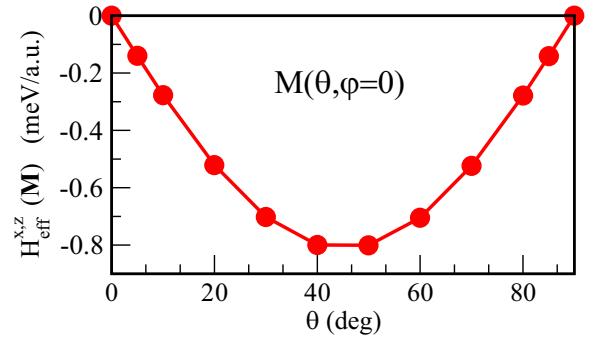


FIG. 9. The dependence of the effective field (closed circles) in bcc Fe on the $\theta$ angle characterizing direction of the magnetization with respect to $\hat{z}$, in the presence of nearest-neighbor displacements along $\hat{z}$ direction, corresponding to a tetragonal distortion of the crystal.

is shown in Fig. 9. Note that in this case the displacement amplitude has been normalized by the factor 1/8 to represent the energy (or field) per one displaced atom. Figure 10 shows the corresponding magnetic torque for $\theta = 45^o$ as a function of the strain, where the SLC-based results (squares) are compared with those of Marchant *et al.* [72]. There are several reasons for the observed deviations: (i) the present results on the MAE are obtained using the nearest-neighbor SLC parameters implying a displacement of only nearest neighbors, in contrast to the volume conserved tetragonal lattice distortion of the bcc lattice in the case of Marchant; (ii) in the later case the electronic structure calculations have been done self-consistently with the torque representing the magnetic anisotropy energy (MAE) $E_{001} - E_{100} = T_{\theta=\pi/4}$.

The MCA-like SLC parameters may be connected with the corresponding magnetoelastic parameter $B_1$ used within micromagnetic considerations (see [54]). On the other hand, the parameter $B_1$ is connected with the magnetostriction constant $\lambda$ representing the relative elongation $\delta l/l$ along the direction of applied magnetic field. For the example considered here the corresponding relation is given by
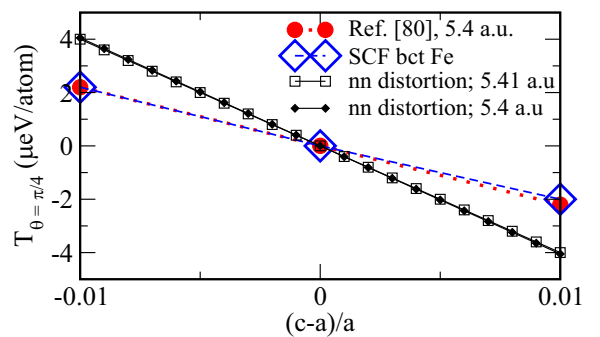
$$B_1 = -\frac{3}{2}\lambda_{001}(C_{11} - C_{12})$$
(33)



FIG. 10. Magnetic torque for magnetization rotated by $\theta = 45^o$ within the $xz$ plane, plotted as a function of strain. The SLC-based results are shown by squares are compared with self-consistent results for the tetragonal distortion of the bcc Fe along [001] direction (diamonds), as well as with corresponding results of Marchant *et al.* [72] (circles).
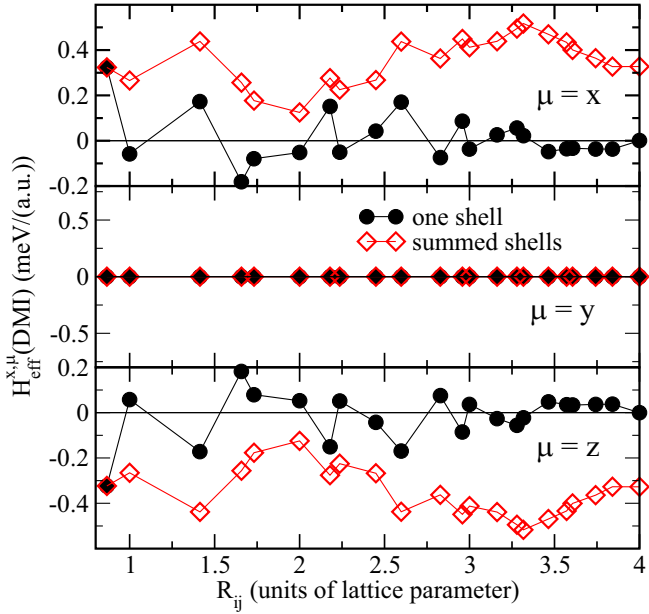
FIG. 11. The shell-resolved effective field for bcc Fe contributed by the DMI-like parameters $\mathcal{D}_{ij,k}^{y,\mu}$, i.e., $-\sum_{j:|R_{ij}|\in d_n}\mathcal{D}_{ij,k}^{y,\mu}$ (closed symbols) up to $|\vec{R}_{ij}^{\max}| = 4a$, accounting for displaced nearest-neighboring atom $k$. Open symbols represent the effective field as a function of $|\vec{R}_{ij}|$ summed up over all contributions up to $|\vec{R}_{ij}|$, i.e., $-\sum_{j:|R_{ij}|\leqslant d_n}\mathcal{D}_{ij,k}^{y,\mu}$. Top panel corresponds to $\mu = x$, middle panel to $\mu = y$, and bottom - to $\mu = z$.



FIG. 12. The shell-resolved effective field for bcc Fe contributed by the diagonal anisotropic part of the SLC tensor, i.e., $\sum_{j:|R_{ij}|\in d_n}1/2(\mathcal{J}_{ij,k}^{xx,\mu} - \mathcal{J}_{ij,k}^{zz,\mu})$ (closed symbols) up to $|\vec{R}_{ij}^{\max}| = 4a$, accounting for displaced nearest-neighboring atom $k$. Open symbols represent the effective field as a function of $|R_{ij}|$ summed up over all contributions up to $|\vec{R}_{ij}|$, i.e., $\sum_{j:|R_{ij}|\in d_n}1/2(\mathcal{J}_{ij,k}^{xx,\mu} - \mathcal{J}_{ij,k}^{zz,\mu})$. The top panel corresponds to $\mu = x$, middle panel to $\mu = y$, and bottom to $\mu = z$.

with the cubic elastic constants $C_{11}$ and $C_{12}$. This implies that the calculation of these elastic parameters is required in addition to compare theoretical results for $B_1$ with experiment.

Note that the effective field considered here is caused by the SOC-induced anisotropic part of the exchange tensor, seen as a nonlocal contribution to the magnetic anisotropy, that concerns also the anisotropy induced by a lattice distortion (via SLC). One should point out that these contributions stem from the DMI-like SLC given by the expression

$$H_i^x(\{\vec{u}_k\}) = \sum_{j,k,\mu}\left(\hat{e}_j \times \vec{D}_{ij,k}^{\mu}\right)_x u_k^{\mu} \qquad (34)$$

(note that the results shown in Figs. 8 and 9 are obtained for $\mu = z$), as well as the anisotropy of the diagonal elements of the SLC tensor $\frac{1}{2}\sum_{j,k}(\mathcal{J}_{ij,k}^{xx,z} - \mathcal{J}_{ij,k}^{zz,z})$. The former one has a dependence on the magnetization direction similar to that of the site-diagonal contribution related to the $\mathcal{K}_{i,k}^{xz,\mu}u_k^{\mu}$ MCA-like term, which is associated to the DMI-like SLC $\vec{\mathcal{D}}_{ij,k}^z$. As one can see in Fig. 9, this contribution vanishes in the case of a tetragonal distortion of the lattice as this deformation does not break inversion symmetry. The effective field associated with the diagonal anisotropy of the SLC tensor is responsible for a uniaxial magnetic anisotropy. It does not vanish in the case of the displacements shown in Fig. 9, as well as in the case of a tetragonal distortion, and is responsible for the nonlocal contribution to the magnetic anisotropy discussed in the literature [15,73].

Discussing the properties of the effective field determined by the three-site SLC parameters (the same concerns also other multisite SLC parameters), one has to take into ac-
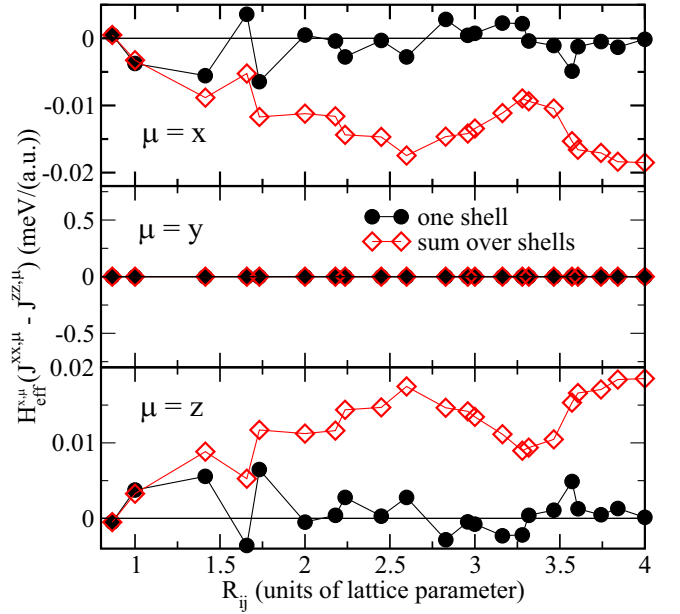
count the $\mathcal{J}_{ij,k}^{\alpha\beta,\mu}$ parameters with $k \neq i$ and $k \neq j$. Thus, their contribution to the effective field (torque) at site $i$ was investigated for the case of a displaced nearest-neighboring atom $k$, but accounting for all SLC contributions including $j \neq k$. Figure 11 shows shell-resolved DMI-SLC contributions to the effective field $H_i^x(u_k^{\mu})$ induced by a displacement $u_k^{\mu}$ of the atom at $\vec{R}_{01} = a(0.5, 0.5, 0.5)$. It is determined by a coupling via the term $\mathcal{D}_{ij,k}^{y,\mu}$ [according to Eq. (34) of the central atom $i$ with all atoms $j$ within the shell $n$ with the radius $d_n$ going up to $d_n^{\max} = |\vec{R}_{ij}^{\max}| = 4a$ (closed symbols). Open symbols represent the sum [using Eq. (34) over all shells around site $i$ up to $d_n = |\vec{R}_{ij}|$. Note that the antisymmetric behavior of these interactions with respect to a permutation of sites $i$ and $j$ ensure a zero total torque on the magnetization due to the vanishing effective field obtained via summation over all sites $i$ in the lattice, assuming fixed positions of the displaced atoms. In a corresponding manner, $|\vec{R}_{ij}|$ dependent results for the effective field due to the diagonal anisotropic part of the SLC tensor, i.e., $\frac{1}{2}\sum_j(\mathcal{J}_{ij,k}^{xx,\mu} - \mathcal{J}_{ij,k}^{zz,\mu})\sin2\theta$, are shown in Fig. 12. However, their absolute value is about an order of magnitude smaller when compared to the effective field associated with the DMI-like SLC.

Following the discussions above on the forces induced via the SLC parameters, $\mathcal{J}_{ij,j}^{\text{dia}-\text{s},\mu}$ and $\mathcal{D}_{ij,j}^{\alpha,\mu}$, one can consider also the force on the atoms on sites $k$ induced via the MCA-like SLC $\mathcal{K}_{i,k}^{\alpha z,\mu}$ by tilting the magnetic moment on site $i$ from the magnetization orientation $\hat{m}||\hat{z}$, as shown schematically in Fig. 13 (left panel). The right panel represents the quantities $\vec{f} = -\sum_\mu \mathcal{K}_{i,k}^{\alpha z,\mu}\hat{n}_\mu$ characterizing forces [see Eq. (31) on
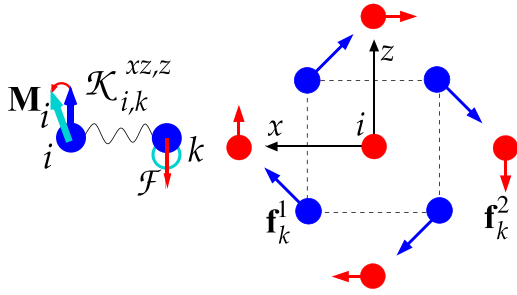
FIG. 13. The quantities $\vec{f} = -\sum_\mu \mathcal{K}_{i,k}^{\alpha z,\mu} \hat{n}_\mu$ ($\hat{n}_x = \hat{x}$, $\hat{n}_y = \hat{y}$, $\hat{n}_z = \hat{z}$) characterizing forces on atoms $j$ induced by spin tilting on site $i$ via the spin-lattice coupling in bcc Fe with the magnetization along $z$ axis. Left panel shows schematically the force $\vec{\mathcal{F}}$ on the atom $k$ (which may be nonmagnetic) induced via $\mathcal{K}_{i,k}^{\alpha z,\mu}$ SLC by tilting of spin moments on site $i$, and vice versa, the spin tiltings induced due to the displacements of atoms on the site $k$. Blue and red arrows show the directions of the forces on atoms $\vec{f}_k^1$ and $\vec{f}_k^2$ within the first and second atomic shells, respectively, assuming spin tilting within the $x - z$ plane, where $\vec{f}_k^1 = (\pm0.69, \pm0.02, \pm0.71)$ (first shell) and $\vec{f}_k^2 = 0.25(0, 0, \pm1)$, $\vec{f}_k^2 = 0.25(0, \pm1, 0)$, $\vec{f}_k^2 = 0.25(\pm1, 0, 0)$ (second shell).

atoms $k$ (corresponding to nearest-neighbor and next-nearest-neighbor atomic shells) induced by a spin tilting on site $i$ via spin-lattice coupling in bcc Fe with the magnetization along $z$ axis. As one can see, these forces are perpendicular to the directions connecting interacting atoms $\hat{R}_{ik}$ similar to the properties of the forces induced via the DMI-like SLC shown in Fig. 3.

One can consider a more complex example with the torque on the magnetic moment generated by phonon-like lattice distortions instead of a single atom displacement. As a reference state, let us consider a FM configuration in the equilibrium, that implies zero total torque on each magnetic moment. Creating a phonon in the system, or, e.g., switching on an external source for acoustic waves, one can expect a distortion in the magnetic structure induced by spin-lattice interactions. This implies that each spin in the FM-ordered system can experience a corresponding torque as a result of the common impact of the displaced surrounding atoms. If the displacement $\vec{u}_j$ is represented in terms of a single phonon mode $\sim e^{i(\vec{q}\cdot\vec{R}_j)}$, the effective field calculated using this Hamiltonian is given by

$$H_{\mathrm{eff},i,\vec{q}}^\alpha = -\frac{\partial}{\partial e_i^\alpha}\mathcal{H}_{\mathrm{me-MA},\vec{q}} = -\sum_\mu K_{i,\vec{q}}^{\alpha z,\mu} e_i^z u_{\vec{q}}^\mu . \quad (35)$$

The other way around, the SLC parameter $K_{i,\vec{q}}^{\alpha z,\mu}$ may be seen as a force acting on the atom on site $i$ when a periodic spin modulation occurs in the FM-ordered system. This way one can see a mutual impact of spin and lattice excitations, which can result in a simultaneous distortion in the system.

## IV. SUMMARY

To summarize, we presented in this paper a scheme to calculate the spin-lattice coupling parameters within the multiple scattering formalism making use of the magnetic force theorem. The properties of the three- and four-site SLC parameters, giving access to the SSC corrections linear and quadratic with respect to displacements, respectively, are discussed. It is demonstrated that the force originating from the DMI-like SLC parameters may be responsible for the mechanical torque on the lattice dependent on the magnetic configuration, that can control the angular momentum transfer via magnon-phonon scattering events. We discussed an approach to calculate the site-diagonal SLC parameters characterizing local magnetic anisotropy induced by a lattice distortion, which is a counterpart to the approach based on magnetic torque calculations worked out for the investigations of the MCA. The approach gives access to all contributions to the MCA-like SLC parameters, accounting also those originating from the anisotropic part of the interatomic SLC parameters. Furthermore, we have demonstrated the contributions of different MCA-like SLC parameters to the energy, considering different types of displacements.

## APPENDIX A: COMPUTATIONAL DETAILS

The results presented in the paper are based on first-principles electronic structure calculations using the spin-polarized relativistic Korringa-Kohn-Rostoker Green's function (SPR-KKR-GF) method [63,74] in combination with atomic sphere approximation (ASA). The local spin density approximation (LSDA) to spin density functional theory (SDFT) has been used with a parametrization for the exchange and correlation potential as given by Vosko *et al.* [75]. The angular momentum expansion of the Green's function was given up to the cutoff $l_{\max} = 3$ was used. A k-mesh with $36 \times 36 \times 36$ grid points was used for the integration over the BZ.

## APPENDIX B: MULTIPLE SCATTERING FORMALISM

Within the KKR Green's function formalism the electronic Green's function $G(\vec{r}, \vec{r}', E)$ is represented in real space by the expression [76]

$$G(\vec{r}, \vec{r}', E) = \sum_{\Lambda_1 \Lambda_2} Z_{\Lambda_1}^n(\vec{r}, E)\tau_{\Lambda_1 \Lambda_2}^{nn'}(E)Z_{\Lambda_2}^{n'\times}(\vec{r}', E)$$

$$- \sum_{\Lambda_1} \left[ Z_{\Lambda_1}^n(\vec{r}, E)J_{\Lambda_1}^{n\times}(\vec{r}', E)\Theta(r' - r) \right.$$

$$\left. + J_{\Lambda_1}^n(\vec{r}, E)Z_{\Lambda_1}^{n\times}(\vec{r}', E)\Theta(r - r') \right]\delta_{nn'} . \quad (B1)$$

Here $\vec{r}, \vec{r}'$ refer to site $n$ and $n'$, respectively, $\tau_{\Lambda\Lambda'}^{nn'}(E)$ is the so-called scattering path operator that transfers an electronic wave coming in at site $n'$ into a wave going out from site $n$ with all possible intermediate scattering events accounted for. The four-component wave functions $Z_\Lambda^n(\vec{r}, E)$ [$J_\Lambda^n(\vec{r}, E)$] are regular [irregular] solutions to the single-site Dirac equation with the Hamiltonian set up within the framework of relativistic spin-density functional theory [77,78],

$$\mathcal{H}_{\mathrm{D}} = -ic\vec{\alpha}\cdot\vec{\nabla} + \tfrac{1}{2}c^2(\beta - 1) + V(\vec{r}) + \beta\vec{\sigma}\cdot\vec{B}_{xc}(\vec{r}) . \quad (B2)$$

These functions are labeled by the combined quantum numbers $\Lambda$ [$\Lambda = (\kappa, \mu)$], with $\kappa$ and $\mu$ being the spin-orbit and magnetic quantum numbers [79]. The superscript $\times$ indicates the left-hand side solution of the Dirac equation. The

operators $\alpha_i$ and $\beta$ in the Hamiltonian in Eq. (B2) are the standard Dirac matrices [79] while $\bar{V}(\vec{r})$ and $\vec{B}_{xc}(\vec{r})$ are the spin independent and dependent parts of the electronic potential [76,79].

## APPENDIX C: CHANGE OF THE INVERSE SCATTERING MATRIX

The change of the inverse scattering matrix due to a spin tilting can be calculated as described earlier in Ref. [16], giving this way direct access to the derivatives with respect to $\hat{e}_i^\alpha$. In this case the change of the inverse scattering matrix $\Delta_\alpha^s \underline{m}_i$ (the underline denotes a matrix in an spin-angular momentum representation $\Lambda$) caused by a tilting of spin moment on site $i$, $\delta \hat{e}_i^\alpha$, can be written as follows [16]:

$$\Delta_\alpha^s \underline{m}_i = \delta \hat{e}_i^\alpha \, \underline{T}_i^\alpha \,, \tag{C1}$$

where the matrix elements $T_{i,\Lambda\Lambda'}^\alpha$ of the torque operator are given by the expression

$$T_{i,\Lambda\Lambda'}^\alpha = \int_{\Omega_i} d^3 r \, Z_\Lambda^{i\times}(\vec{r}, E) \left[ \beta \sigma_\alpha B_{xc}^i(\vec{r}) \right] Z_{\Lambda'}^i(\vec{r}, E) \,, \tag{C2}$$

with $\mu = (x, y, z)$. Note that using the fixed frame of reference with the magnetization along $z$ axis, only the two torque components $\underline{T}_i^x$ and $\underline{T}_i^y$ linear with respect to the tilting angle are available. To get access to the other component $\underline{T}_i^z$, one has to use a rotated frame of reference as it was suggested by

Udvardi *et al.* [15] when introducing relativistic calculations of the exchange coupling tensor $\underline{J}_{ij}$.

In the case of atom $i$ displaced from the equilibrium position by $\vec{u}_i$, the change of the single-site scattering matrix $\Delta \underline{t}_i = \underline{t}_i - \underline{t}_i^0$ is given in terms of the $t$-matrix $\underline{t}_i^{(0)}$ for the unshifted atom, and the scattering matrix for shifted atom

$$\underline{t}_i = \underline{U}(\vec{u}_i) \, \underline{t}_i^0 \, \underline{U}(\vec{u}_i)^{-1} \,, \tag{C3}$$

(analogously for the inversed scattering matrices $\underline{m}_i^0$ and $\underline{m}_i$), where the transformation matrix $\underline{U}_i$ is given by the expression [80,81]

$$U_{LL'}(\vec{u}_i) = 4\pi \sum_{L''} i^{l+l''-l'} C_{LL'L''} j_{l''}(|\vec{u}_i|k) \mathcal{Y}_{L''}(\hat{u}_i), \tag{C4}$$

given here in the nonrelativistic form with $k = \sqrt{2mE/\hbar^2}$, and $\mathcal{Y}_L$ real spherical harmonics. In Eq. (C4) $j_l$ is a spherical Bessel function, $C_{LL'L''}$ stands for the Gaunt coefficients given in nonrelativistic angular momentum representation with $L = (l, m_l)$. The relativistic form of $U_{k,\Lambda\Lambda'}$ is obtained by a standard Clebsch-Gordan transformation. The inversed transformation matrix can be written as follows:

$$[U^{-1}(\vec{u}_i)]_{LL'} = \qquad U_{LL'}(-\vec{u}_i) = U_{L'L}(\vec{u}_i). \tag{C5}$$

The Bessel function $j_{l''}(|\vec{u}_i|k)$ in the limit of a small displacement amplitude $|\vec{u}_i|$ is given by the expression [82]

$$j_l(|\vec{u}_i|k) = \frac{(|\vec{u}_i|k)^l}{(2l+1)!!} \,. \tag{C6}$$

Keeping in Eq. (C4) only the terms up to second order with respect to the displacement, one obtains

$$U_{LL'}(\vec{u}_i) = 4\pi \sum_{L''} i^{l+l''-l'} C_{LL'L''} \frac{(|\vec{u}_i|k)^{l''}}{(2l''+1)!!} \mathcal{Y}_{L''}(\hat{u}_i) = 4\pi \left[ i^{l+0-l'} C_{LL'00} \frac{(|\vec{u}_i|k)^0}{(1)!!} \mathcal{Y}_{00}(\hat{u}_i) \right.$$

$$+ \sum_{m=-1}^{1} i^{l+1-l'} C_{LL'1m} \frac{(|\vec{u}_i|k)^1}{(3)!!} \mathcal{Y}_{1m}(\hat{u}_i) + \sum_{m=-2}^{2} i^{l+2-l'} C_{LL'2m} \frac{(|\vec{u}_i|k)^2}{(5)!!} \mathcal{Y}_{2m}(\hat{u}_i) + \ldots \right]$$

$$= 4\pi \left[ i^{l-l'} \frac{1}{\sqrt{4\pi}} 1 \frac{1}{\sqrt{4\pi}} \delta_{LL'} + i^{l+1-l'} \sum_{m=-1}^{1} C_{LL'1m} \frac{|\vec{u}_i|k}{(3)} \mathcal{Y}_{1m}(\hat{u}_i) \right.$$

$$\left. + i^{l+2-l'} \sum_{m=-2}^{2} C_{LL'2m} \frac{|\vec{u}_i|^2 k^2}{15} C_{l0,l'0,20}^{-1} \left( \sqrt{\frac{20\pi}{9}} \sum_{m_1=-1}^{1} \sum_{m_2=-1}^{1} C_{1m_1,1m_2,2m} \mathcal{Y}_{1m_1}(\hat{u}_i) \mathcal{Y}_{1m_2}(\hat{u}_i) \right) + \ldots \right]$$

$$\approx \delta_{LL'} + \frac{4\pi}{3} |\vec{u}_i| k \, i^{l+1-l'} \sum_{m=-1}^{1} C_{LL'1m} \mathcal{Y}_{1m}(\hat{u}_i)$$

$$+ \frac{4\pi}{15} \sqrt{\frac{20\pi}{9}} |\vec{u}_i|^2 k^2 i^{l+2-l'} \sum_{m=-2}^{2} C_{LL'2m} C_{l0,l'0,20}^{-1} \left( \sum_{m_1=-1}^{1} \sum_{m_2=-1}^{1} C_{1m_1,1m_2,2m} \mathcal{Y}_{1m_1}(\hat{u}_i) \mathcal{Y}_{1m_2}(\hat{u}_i) \right) + \ldots$$

where the following expansion is used [82]

$$C_{l0,l'0,20} \mathcal{Y}_{lm}(\hat{u}_i) = \sqrt{\frac{4\pi(2l+1)}{(2l_1+1)(2l_2+1)}} \sum_{m_1=-l_1}^{l_1} \sum_{m_2=-l_2}^{l_2} C_{l_1m_1,l_2m_2,2m} \mathcal{Y}_{lm_1}(\hat{u}_i) \mathcal{Y}_{1m_2}(\hat{u}_i)$$

Here the direction of displacement of atom $i$ is given by unit vector $\hat{u}_i$.

Representing the real spherical harmonics $\mathcal{Y}_{1m}(\hat{u}_i)$ in the following form:

$$\mathcal{Y}_{1m}(\hat{u}_i) = \sqrt{\frac{3}{4\pi}} \begin{cases} u_i^y/|\vec{u}_i| = \hat{u}_i^y & \text{for } m = -1 \\ u_i^z/|\vec{u}_i| = \hat{u}_i^z & \text{for } m = 0 \\ u_i^x/|\vec{u}_i| = \hat{u}_i^x & \text{for } m = +1 \end{cases}$$

the transformation functions $U_{LL'}(\vec{u}_i)$ is reduced to the following form:

$$U_{LL'}(\vec{u}_i) \approx \delta_{LL'} + \sum_\mu \frac{4\pi}{3}\sqrt{\frac{3}{4\pi}} u_i^\mu k i^{l+1-l'} C_{LL'1m_\mu}$$

$$+ \sum_\mu \sum_\nu^1 \frac{4\pi}{15}\sqrt{\frac{20\pi}{9}}\frac{3\cdot 2}{4\pi} u_i^\mu u_i^\nu k^2 i^{l+2-l'} \sum_{m=-2}^2 C_{LL'2m} C_{l0,l'0,20}^{-1} C_{1m_\mu,1m_\nu,2m} + \dots$$

$$= \delta_{LL'} + \sum_\mu u_i^\mu \bar{U}_{LL'}^{m_\mu} + \sum_{\mu\nu} u_i^\mu u_i^\nu \bar{U}_{LL'}^{(2b),m_\mu m_\nu},$$

$$U_{LL'}(-\vec{u}_i) \approx \delta_{LL'} - \sum_\mu u_i^\mu \bar{U}_{LL'}^{m_\mu} + \sum_{\mu\nu} u_i^\mu u_i^\nu \bar{U}_{LL'}^{(2b),m_\mu m_\nu},$$

where $m_{\mu(\nu)} = \{m_x, m_y m_z\}$, such that $m_x = 1$, $m_y = -1$, $m_z = 0$,

$$\bar{U}_{LL'}^{m_x} = k\frac{4\pi}{3} i^{l-l'+1}\sqrt{\frac{3}{4\pi}} C_{LL'1\,+1} = k i^{l-l'+1}\sqrt{\frac{4\pi}{3}} C_{LL'1\,+1},$$

$$\bar{U}_{LL'}^{m_y} = k i^{l-l'+1}\sqrt{\frac{4\pi}{3}} C_{LL'1\,-1},$$

$$\bar{U}_{LL'}^{m_z} = k i^{l-l'+1}\sqrt{\frac{4\pi}{3}} C_{LL'1\,0},$$

$$\bar{U}_{LL'}^{2b,\mu\nu} \equiv \bar{U}_{LL'}^{2b,m_\mu m_\nu} = k^2 \frac{1}{3}\sqrt{\frac{4\pi}{5}} i^{l+2-l'} \sum_{m=-2}^2 C_{LL'2m} C_{l0,l'0,20}^{-1} C_{1m_\mu,1m_\nu,2m},$$

where

$$\bar{U}_{LL'}^\mu(-\hat{u}_i) = -\bar{U}_{LL'}^\mu(\hat{u}_i), \quad \bar{U}_{LL'}^{2b,\mu\nu}(-\hat{u}_i) = \bar{U}_{LL'}^{2b,\mu\nu}(\hat{u}_i),$$

as a consequence of the property

$$\mathcal{Y}_{1m}(-\hat{u}_i) = (-1)^1 \mathcal{Y}_{1m}(\hat{u}_i) = -\mathcal{Y}_{1m}(\hat{u}_i).$$

Thus, we obtain the approximate transformation matrix for a small displacement $\vec{u}_i^\mu$,

$$U_{LL'}(\vec{u}_i) = \delta_{LL'} + \sum_\mu u_i^\mu \bar{U}_{LL'}^{m_\mu} + \sum_{\mu,\nu} u_i^\mu u_i^\nu \bar{U}_{LL'}^{(2b),m_\mu m_\nu}, \tag{C7}$$

or, using the notation $\bar{U}_{LL'}^{(2b),\mu\nu} \equiv \bar{U}_{LL'}^{(2b),m_\mu m_\nu}$, one can represent the modified single-site scattering matrix as follows:

$$\tilde{\underline{t}}_i = \underline{U}(\vec{u}_i)\,\underline{t}_i\,\underline{U}^{-1}(\vec{u}_i) = \underline{U}(\vec{u}_i)\,\underline{t}_i\,\underline{U}(-\vec{u}_i)$$

$$\approx \left(\underline{I} + \sum_{\mu'} u_i^{\mu'}\,\underline{\bar{U}}^{\mu'}(\hat{u}_i) + \sum_{\mu'\nu'} u_i^{\mu'} u_i^{\nu'}\,\underline{\bar{U}}^{(2b),\mu'\nu'}(\hat{u}_i)\right)\underline{t}_i\left(\underline{I} + \sum_{\nu''} u_i^{\nu''}\,\underline{\bar{U}}^{\mu''}(-\hat{u}_i) + \sum_{\mu''\nu''} u_i^{\mu''} u_i^{\nu''}\,\underline{\bar{U}}^{(2b),\mu''\nu''}(-\hat{u}_i)\right)$$

$$\approx \underline{t} + \sum_\mu \left(u_i^\mu\,\bar{U}^\mu(\hat{u}_i)\,\underline{t}_i + u_i^\mu\,\underline{t}_i\,\bar{U}^\mu(-\hat{u}_i)\right)$$

$$+ \sum_{\mu\nu} u_i^\mu u_i^\nu \left(\bar{U}^\mu(\hat{u}_i)\,\underline{t}_i\,\bar{U}^\nu(-\hat{u}_i) + \bar{U}(\hat{u}_i^\nu)\,\underline{t}_i\,\bar{U}(-\hat{u}_i^\mu) + \underline{\bar{U}}^{(2b),\mu\nu}(\hat{u}_i)\underline{t}_i + \underline{t}_i\,\underline{\bar{U}}^{(2b),\mu\nu}(-\hat{u}_i)\right),$$

$$\tilde{\underline{t}}_i - \underline{t}_i = \sum_\mu u_i^\mu \left(\bar{U}^\mu(\hat{u}_i)\,\underline{t}_i - \underline{t}_i\,\bar{U}^\mu(\hat{u}_i)\right) + \sum_{\mu\nu} u_i^\mu u_i^\nu \left(-\bar{U}^\mu(\hat{u}_i)\,\underline{t}_i\,\bar{U}^\nu(\hat{u}_i) - \bar{U}^\nu(\hat{u}_i)\,\underline{t}_i\,\bar{U}^\mu(\hat{u}_i) + \underline{\bar{U}}^{(2b),\mu\nu}(\hat{u}_i)\underline{t}_i\right.$$

$$\left. + \underline{t}_i\,\underline{\bar{U}}^{(2b),\mu\nu}(\hat{u}_i)\right) + O((u_i^\mu)^3), \tag{C8}$$

and analogously for $m_i = t_i^{-1}$.

## APPENDIX D: TORQUE ON MAGNETIC MOMENT

Here we give the relationship between the torque on a magnetic moment of the system and the energy change due to a rotation of the magnetic moment, that is used for the calculations of the magnetocrystalline anisotropy energy in magnetic systems [56]. Let us consider a FM-ordered system with the magnetization direction $\hat{e}$. The energy change due to a tilting of the magnetic moment is given by the expression

$$\delta E = \frac{\delta E}{\delta \hat{e}} \cdot \delta \hat{e} = \frac{\delta E}{\delta \hat{e}} \cdot \vec{\delta\theta} \times \hat{e} \tag{D1}$$

$$= -\vec{H}_{\text{eff}} \cdot [\vec{\delta\theta} \times \hat{e}] = -\vec{\delta\theta} \cdot [\hat{e} \times \vec{H}_{\text{eff}}] \tag{D2}$$

$$= -\delta\theta \, \hat{n} \cdot [\hat{e} \times \vec{H}_{\text{eff}}] = -\delta\theta \, T^{\hat{n}} \tag{D3}$$

with the effective field $\vec{H}_{\text{eff}} = -\frac{\delta E}{\delta \hat{e}}$, $\delta\hat{e} = \vec{\delta\theta} \times \hat{e}$, $\vec{\delta\theta} = \hat{n}\delta\theta$, and $\hat{n}$ the direction perpendicular to the plane of rotation by the angle $\delta\theta$ of the magnetization direction. Thus, the torque on the magnetic moment represented in terms of local effective field

$$\vec{T} = \hat{e} \times \vec{H}_{\text{eff}} \tag{D4}$$

gives access to the MCA energy via its projection on the direction $\hat{n}$

$$T^{\hat{n}}(\hat{e}) = \hat{n} \cdot [\hat{e} \times \vec{H}_{\text{eff}}] \tag{D5}$$

characterizing the energy change due to a rotation of the magnetization. Representing this direction in terms of the polar angles $\theta$ and $\phi$, the torque may be defined as the derivative

$$T^{\hat{n}}(\hat{e}) = -\frac{\partial E}{\partial \theta}. \tag{D6}$$

As it was discussed in Refs. [15,56], this quantity can be used for the calculation of the magnetic anisotropy parameters. In particular, considering the magnetization direction tilted by $\theta = \pi/4$, the corresponding torque $T^{\hat{n}}(\pi/4)$ gives direct access to the energy of uniaxial anisotropy $T^{\hat{n}}(\pi/4) = E(\hat{e}||\hat{x}) - E(\hat{e}||\hat{z})$, and as a consequence to the uniaxial anisotropy parameters.

[1] S. Polesya, S. Mankovsky, O. Šipr, W. Meindl, C. Strunk, and H. Ebert, Phys. Rev. B **82**, 214409 (2010).

[2] B. Skubic, J. Hellsvik, L. Nordström, and O. Eriksson, J. Phys.: Condens. Matter **20**, 315203 (2008).

[3] H. Capellmann, J. Phys. F **4**, 1466 (1974).

[4] R. E. Prange and V. Korenman, Phys. Rev. B **19**, 4691 (1979).

[5] C. S. Wang, R. E. Prange, and V. Korenman, Phys. Rev. B **25**, 5766 (1982).

[6] T. Oguchi, K. Terakura, and A. R. Williams, Phys. Rev. B **28**, 6443 (1983).

[7] A. I. Liechtenstein, M. I. Katsnelson, V. P. Antropov, and V. A. Gubanov, J. Magn. Magn. Mater. **67**, 65 (1987).

[8] V. Antropov, M. Katsnelson, and A. Liechtenstein, Phys. B: Condens. Matter **237-238**, 336 (1997).

[9] M. Uhl, L. M. Sandratskii, and J. Kübler, Phys. Rev. B **50**, 291 (1994).

[10] V. P. Antropov, M. van Schilfgaarde, S. Brink, and J. L. Xu, J. Appl. Phys. **99**, 08F507 (2006).

[11] A. Antal, B. Lazarovits, L. Udvardi, L. Szunyogh, B. Újfalussy, and P. Weinberger, Phys. Rev. B **77**, 174429 (2008).

[12] M. Heide, G. Bihlmayer, and S. Blügel, Phys. Rev. B **78**, 140403(R) (2008).

[13] S. Mankovsky and H. Ebert, Electron. Struct. **4**, 034004 (2022).

[14] A. Szilva, Y. Kvashnin, E. A. Stepanov, L. Nordström, O. Eriksson, A. I. Lichtenstein, and M. I. Katsnelson, arXiv:2206.02415.

[15] L. Udvardi, L. Szunyogh, K. Palotás, and P. Weinberger, Phys. Rev. B **68**, 104436 (2003).

[16] H. Ebert and S. Mankovsky, Phys. Rev. B **79**, 045209 (2009).

[17] S. Brinker, M. dos Santos Dias, and S. Lounis, New J. Phys. **21**, 083015 (2019).

[18] S. Mankovsky, S. Polesya, and H. Ebert, Phys. Rev. B **101**, 174401 (2020).

[19] S. Lee, A. Pirogov, M. Kang, K.-H. Jang, M. Yonemura, T. Kamiyama, S.-W. Cheong, F. Gozzo, N. Shin, H. Kimura et al., Nature (London) **451**, 805 (2008).

[20] K. Kimura, T. Otani, H. Nakamura, Y. Wakabayashi, and T. Kimura, J. Phys. Soc. Jpn. **78**, 113710 (2009).

[21] J. C. E. Rasch, M. Boehm, C. Ritter, H. Mutka, J. Schefer, L. Keller, G. M. Abramova, A. Cervellino, and J. F. Löffler, Phys. Rev. B **80**, 104431 (2009).

[22] K. Singh, A. Maignan, C. Martin, and C. Simon, Chem. Mater. **21**, 5007 (2009).

[23] K. Takeda, K. Miyake, M. Hitaka, T. Kawae, N. Yaguchi, and M. Mekata, J. Phys. Soc. Jpn. **63**, 2017 (1994).

[24] F. Wang and A. Vishwanath, Phys. Rev. Lett. **100**, 077201 (2008).

[25] K. Park, J. Oh, J. C. Leiner, J. Jeong, K. C. Rule, M. D. Le, and J.-G. Park, Phys. Rev. B **94**, 104421 (2016).

[26] J. Oh, M. D. Le, H.-H. Nahm, H. Sim, J. Jeong, T. G. Perring, H. Woo, K. Nakajima, S. Ohira-Kawamura, Z. Yamani et al., Nat. Commun. **7**, 13146 (2016).

[27] T. Kim, K. Park, J. C. Leiner, and J.-G. Park, J. Phys. Soc. Jpn. **88**, 081003 (2019).

[28] E. Beaurepaire, J.-C. Merle, A. Daunois, and J.-Y. Bigot, Phys. Rev. Lett. **76**, 4250 (1996).

[29] B. Vodungbo, J. Gautier, G. Lambert, A. B. Sardinha, M. Lozano, S. Sebban, M. Ducousso, W. Boutu, K. Li, B. Tudu et al., Nat. Commun. **3**, 999 (2012).

[30] J. Gorchon, R. B. Wilson, Y. Yang, A. Pattabi, J. Y. Chen, L. He, J. P. Wang, M. Li, and J. Bokor, Phys. Rev. B **94**, 184406 (2016).

[31] M. Fähnle, T. Tsatsoulis, C. Illg, M. Haag, B. Y. Müller, and L. Zhang, J. Supercond. Novel Magn. **30**, 1381 (2017).

[32] J. J. Nakane and H. Kohno, Phys. Rev. B **97**, 174403 (2018).

[33] J. H. Mentink, M. I. Katsnelson, and M. Lemeshko, Phys. Rev. B **99**, 064428 (2019).

[34] C. Dornes, Y. Acremann, M. Savoini, M. Kubli, M. J. Neugebauer, E. Abreu, L. Huber, G. Lantz, C. A. F. Vaz, H. Lemke et al., Nature (London) **565**, 209 (2019).

[35] M. Xu, J. Puebla, F. Auvray, B. Rana, K. Kondou, and Y. Otani, Phys. Rev. B **97**, 180301(R) (2018).

[36] N. Ogawa, W. Koshibae, A. J. Beekmana, N. Nagaosa, M. Kubota, M. Kawasaki, and Y. Tokura, Proc. Natl. Acad. Sci. USA **112**, 8977 (2015).

[37] R. John, M. Berritta, D. Hinzke, C. Müller, T. Santos, H. Ulrichs, P. Nieves, J. Walowski, R. Mondal, O. Chubykalo-Fesenko *et al.*, Sci. Rep. **7**, 4114 (2017).

[38] A. Stupakiewicz, C. S. Davies, K. Szerenos, D. Afanasiev, K. S. Rabinovich, A. V. Boris, A. Caviglia, A. V. Kimel, and A. Kirilyuk, Nat. Phys. **17**, 489 (2021).

[39] C. Kittel, Phys. Rev. **110**, 836 (1958).

[40] E. Schlömann, J. Appl. Phys. **31**, 1647 (1960).

[41] A. G. Gurevich and G. A. Melkov, *Magnetization Oscillations and Waves* (CRC Press, Boca Raton, FL, 1996).

[42] S. Mankovsky, S. Polesya, H. Ebert, W. Bensch, O. Mathon, S. Pascarelli, and J. Minár, Phys. Rev. B **88**, 184108 (2013).

[43] K. Yin, P. Gao, X. Shao, B. Gao, H. Liu, J. Lv, J. S. Tse, Y. Wang, and Y. Ma, npj Comput. Mater. **6**, 16 (2020).

[44] J. Yin, M. Eisenbach, D. M. Nicholson, and A. Rusanu, Phys. Rev. B **86**, 214423 (2012).

[45] A. V. Ruban and O. E. Peil, Phys. Rev. B **97**, 174426 (2018).

[46] F. Körmann, B. Grabowski, B. Dutta, T. Hickel, L. Mauger, B. Fultz, and J. Neugebauer, Phys. Rev. Lett. **113**, 165503 (2014).

[47] P.-W. Ma, C. H. Woo, and S. L. Dudarev, Phys. Rev. B **78**, 024434 (2008).

[48] D. Perera, M. Eisenbach, D. M. Nicholson, G. M. Stocks, and D. P. Landau, Phys. Rev. B **93**, 060402(R) (2016).

[49] M. Aßmann and U. Nowak, J. Magn. Magn. Mater. **469**, 217 (2019).

[50] M. Strungaru, M. O. A. Ellis, S. Ruta, O. Chubykalo-Fesenko, R. F. L. Evans, and R. W. Chantrell, Phys. Rev. B **103**, 024429 (2021).

[51] J. Hellsvik, D. Thonig, K. Modin, D. Iuşan, A. Bergman, O. Eriksson, L. Bergqvist, and A. Delin, Phys. Rev. B **99**, 104302 (2019).

[52] B. Sadhukhan, A. Bergman, Y. O. Kvashnin, J. Hellsvik, and A. Delin, Phys. Rev. B **105**, 104418 (2022).

[53] S. Mankovsky, S. Polesya, H. Lange, M. Weißenhofer, U. Nowak, and H. Ebert, Phys. Rev. Lett. **129**, 067202 (2022).

[54] M. Weißenhofer, H. Lange, A. Kamra, S. Mankovsky, S. Polesya, H. Ebert, and U. Nowak, arXiv:2211.02382.

[55] X. Wang, D. Wang, R. Wu, and A. J. Freeman, J. Magn. Magn. Mater. **159**, 337 (1996).

[56] J. B. Staunton, L. Szunyogh, A. Buruzs, B. L. Gyorffy, S. Ostanin, and L. Udvardi, Phys. Rev. B **74**, 144411 (2006).

[57] H. Lange, S. Mankovsky, S. Polesya, M. Weißenhofer, U. Nowak, and H. Ebert, Phys. Rev. B **107**, 115176 (2023).

[58] O. Grotheer, C. Ederer, and M. Fähnle, Phys. Rev. B **63**, 100401(R) (2001).

[59] V. Antropov, J. Magn. Magn. Mater. **262**, L192 (2003).

[60] P. Bruno, Phys. Rev. Lett. **90**, 087205 (2003).

[61] I. V. Solovyev, Phys. Rev. B **103**, 104428 (2021).

[62] J. Kübler, *Theory of Itinerant Electron Magnetism* (Oxford University Press, Oxford, 2000) p. 460.

[63] H. Ebert, D. Ködderitzsch, and J. Minár, Rep. Prog. Phys. **74**, 096501 (2011).

[64] D. A. Garanin and E. M. Chudnovsky, Phys. Rev. B **92**, 024421 (2015).

[65] A. Rückriegel, S. Streib, G. E. W. Bauer, and R. A. Duine, Phys. Rev. B **101**, 104402 (2020).

[66] S. Mankovsky, S. Polesya, and H. Ebert, Phys. Rev. B **102**, 134434 (2020).

[67] S. J. Allen and H. J. Guggenheim, Phys. Rev. B **4**, 937 (1971).

[68] J. B. Torrance and J. C. Slonczewski, Phys. Rev. B **5**, 4648 (1972).

[69] E. N. Economou, K. L. Ngai, T. L. Reinecke, J. Ruvalds, and R. Silberglitt, Phys. Rev. B **13**, 3135 (1976).

[70] E. W. Lee, Rep. Prog. Phys. **18**, 184 (1955).

[71] C. Kittel and E. Abrahams, Rev. Mod. Phys. **25**, 233 (1953).

[72] G. A. Marchant, C. E. Patrick, and J. B. Staunton, Phys. Rev. B **99**, 054415 (2019).

[73] S. Mankovsky, S. Polesya, S. Bornemann, J. Minár, F. Hoffmann, C. H. Back, and H. Ebert, Phys. Rev. B **84**, 201201(R) (2011).

[74] H. Ebert *et al.*, *The Munich SPR-KKR package*, version 8.5, https://www.ebert.cup.uni-muenchen.de/en/software-en/13-sprkkr (2020).

[75] S. H. Vosko, L. Wilk, and M. Nusair, Can. J. Phys. **58**, 1200 (1980).

[76] H. Ebert, J. Braun, D. Ködderitzsch, and S. Mankovsky, Phys. Rev. B **93**, 075145 (2016).

[77] A. H. MacDonald and S. H. Vosko, J. Phys. C: Solid State Phys. **12**, 2977 (1979).

[78] E. Engel and R. M. Dreizler, *Density Functional Theory–An advanced course* (Springer, Berlin, 2011).

[79] M. E. Rose, *Relativistic Electron Theory* (Wiley, New York, 1961).

[80] N. Stefanou, P. J. Braspenning, R. Zeller, and P. H. Dederichs, Phys. Rev. B **36**, 6372 (1987).

[81] N. Papanikolaou, R. Zeller, P. H. Dederichs, and N. Stefanou, Phys. Rev. B **55**, 4157 (1997).

[82] M. E. Rose, *Elementary Theory of Angular Momentum* (Wiley, New York, 1957).